

Preface

This thesis was written for the course TMT4900 as the last part of my M.Sc. degree in Material Sciences at the Norwegian University of Science and Technology, during the spring semester of 2022.

First I would like to express my gratitude to my supervisor professor Gabriella Tranell and co-supervisor PhD candidate Azam Rasouli. This project has not been without problems or difficulties, your guidance and competence has been very helpful and I am very grateful for the amount of time you have invested into me and my project. You have introduced me to the large field of silicon and sparked a passion that will now be pursued as a career path. I hope that we will meet again in the future either through work or academia. For Azam I wish you "lykke til" on your continued papers and Norwegian studies.

I am very grateful for the time at NTNU and I would like to dedicate the last paragraph to the people whom I consider some of my best friends. Vemund, Amund, Henning, Markus, Brynjar, Torgeir, Erlend and Nishan, I am grateful for all the great times we have spent together during our studies and I am sure that there are more to come.

Trondheim, April 2022.

Karl Edvin Herstad

Abstract

The aim of this project has been to develop a method for liquid analysis of the gas products formed through the chemical reaction between Mg_2Si and HCl . An original reaction setup utilizing the reactivity between silane gas and aqueous KOH has been developed and used for quantitative and qualitative measurements. Silane gas has been produced locally and captured by the use of a gas bubbler filled with KOH , and the reaction products have been analysed by the use of ICP-MS, XRD and SEM.

Different reaction parameters such as amount of Mg_2Si , HCl concentration, KOH concentration and size of gas bubbles have been varied to investigate the effect on silane gas production and capture ability of the KOH solution. The method of analysis was implemented and found to be able to quantify the amount of silane gas produced. The reaction between Mg_2Si and HCl was found to produce silane gases as well as a significant amount of solid product found to be a mix of Si and amorphous silica. From the silane gases produced a maximum yield of 21% silicon as silane was achieved from the original amount in Mg_2Si .

The developed method was found to be a viable option in quantifying the amount of silane gas as an alternative to advanced gas analysis equipment. The KOH solution was found to capture silane gas more effectively by increased strength of KOH . By increasing the surface area of the gas bubbles with a porous bubbler a further increase in silicon capture was observed.

Sammendrag

Målet med dette prosjektet har vært å utvikle en metode for væskeanalyse av gassproduktene produsert gjennom den kjemiske reaksjonen mellom Mg_2Si og HCl . Et originalt reaksjonsoppsett som utnytter reaktiviteten mellom silangass og KOH i løsning har blitt utviklet for kvantitative og kvalitative målinger. Silangass har blitt produsert lokalt og tatt opp gjennom bruk av en gassbobler fylt med en KOH -løsning, og reaksjonsproduktene har blitt analysert gjennom bruk av ICP-MS, XRD og SEM.

Ulike reaksjonsparametere slik som mengde Mg_2Si , HCl -konsentrasjon, KOH -konsentrasjon og størrelse på gassbobler har blitt variert for å undersøke effekten på produksjon av silangass og opptaksevnen til KOH -løsningen. Analysemetoden var implementert og funnet i stand til å kvantifisere mengden silangass produsert. Reaksjonen mellom Mg_2Si og HCl produserte silangass i tillegg til betydelige mengder presipitat som ble funnet til å bestå av Si og amorf silika. Fra silangassene produsert ble det maksimale utbyttet funnet til å være 21% silisium som silan basert på den opprinnelige mengden i Mg_2Si .

Den utviklede metoden er funnet i stand til å være et godt verktøy for å kvantifisere silangass alternativt til avanserte gassanalyseinstrumenter. KOH -løsningen reagerte med silangass mere effektivt med økt styrke på KOH -løsningen. Ved å øke overflatearealet av gassboblene med en porøs bobler ble det oppdaget en videre økning i fangstgrad.

Contents

Contents	iv
List of Figures	vii
List of Tables	ix
1 Introduction	1
1.1 Background and motivation	1
1.2 Scope of the thesis	2
2 Theory and Literature study	4
2.1 Silicon application and production	4
2.1.1 Global production and areas of application	6
2.1.2 Carbothermic reduction	6
2.1.3 Production disadvantages and climate aspect	9
2.2 Metallothermic reduction	11
2.2.1 Aluminothermic reduction and the SisAl process	13
2.2.2 Magnesiothermic reduction	14
2.3 Upgrading to SoG-Si	15
2.3.1 Chemical route: Siemens process	16
2.3.2 Chemical route: Fluidized Bed Reactor	17
2.4 Silane properties and use in SoG-Si production	19
2.4.1 SiH_4	20
2.4.2 Oxidation of SiH_4	23
2.5 Literature survey	24
3 Experimental procedure	32
3.1 Material	32
3.2 Experimental design	32
3.3 Procedure	33
3.3.1 KOH concentration	36
3.3.2 Bubbler porosity	37

3.3.3	Amount of Mg ₂ Si	37
3.3.4	HCl concentration	39
3.3.5	Precipitate	39
3.4	Characterisation	39
3.4.1	Sample preparation	40
4	Results	43
4.1	KOH concentration	43
4.2	Bubbler porosity	46
4.3	Amount of Mg ₂ Si	48
4.4	HCl concentration	50
4.4.1	HCl residue	50
4.5	Observations	56
5	Discussion	60
5.1	Variation of reaction parameters	60
5.1.1	KOH concentration	61
5.1.2	Porous bubbler	63
5.1.3	Increasing amount of Mg ₂ Si	65
5.1.4	Concentration of HCl	65
5.2	Observations	66
5.2.1	Preliminary experiments	66
5.2.2	SiO ₂ dust formation	67
5.3	Analysis	67
5.3.1	HCl solutions	67
5.3.2	X-ray powder diffraction and Scanning Electron Mi- croscopy	68
5.3.3	Dilution of samples	68
5.4	Method feasibility	69
5.5	Reaction parameters	70
6	Conclusion	71
6.1	Future work	72

7	References	73
A	Calculation of Si yield	77

List of Figures

1	Flow chart of a possible alternative route for producing high purity silicon for solar applications.	3
2	Solar electricity generation cost in comparison with other power sources in the period 2009 - 2020 ^[1]	5
3	Top 10 solar PV markets in the period 2019-2020 ^[1]	6
4	A standard silicon plant showing the process from raw material to final product ^[2]	8
5	Ellingham diagram showing the stability of various metal oxides ^[3]	12
6	Impurity concentration limits in p-type Si determining the reduction in efficiency of solar cells: (1) EG-Si, (2) SoG-Si and (3) MG-Si ^[4]	16
7	(a) Basic Siemens reactor. (b) As grown polysilicon rods after a reactor run. Current generation reactors have many more rods. (c) Final polysilicon chunks ^[5]	18
8	Mechanism of acidic hydrolysis of Mg ₂ Si into monosilane.	21
9	Graphs showing the simulated enthalpy and Gibbs energy curves for the reaction between Mg ₂ Si and HCl.	22
10	Relationship between silicon yield in the form of silane gas at different HCl concentrations (v/v%) ^[6]	25
11	Relationship between silicon yield and silane ratio against increase in reaction temperature (°C) ^[6]	26
12	Caption	27
13	Gas characterization of the reaction between Mg ₂ Si and NH ₄ F by mass spectrometry ^[7]	29
14	Flowsheet showing the reaction setup used in the experiments. (1.) Argon bottle 99.999%, (2.) Alicat mass flow controller, (3.) Glass dropping funnel, (4.) Glass Erlenmeyer flask (inlet/outlet) and (5.) Glass gas bubbler.	34
15	Comparison between porous bubbler "level 0" (left) and standard bubbler (right).	38

16	Si content collected in real and blank solution for experiments done with increasing molarity of KOH, corresponding yield to the real experiments are shown in separate y-axis.	45
17	Silicon content collected in increased concentrations of KOH in the porous bubbler compared to the standard bubbler. Corresponding Si yield comparison when compared to original Mg ₂ Si samples of 300 mg is shown at separate y-axis.	47
18	Si content and corresponding yield for experiments done with increasing amount of Mg ₂ Si by the use of the porous bubbler with constant concentration of 2 mol L ⁻¹ KOH.	49
19	Si content and corresponding yield for experiments done with increasing concentration of HCl by the use of the porous bubbler with constant concentration of 2 mol L ⁻¹ KOH.	51
20	XRD plot of experiment 14, indicated peaks correspond to that of Si and amorphous SiO ₂	53
21	XRD plot of the Mg ₂ Si powder used for the experiments, indicated peaks correspond to that of Mg ₂ Si.	54
22	Secondary electron imaging of experiment 17 HCl residue at 2000X magnification.	55
23	Backscattered electron imaging of experiment 17 HCl residue at 1000X magnification.	56
25	Formation of white coating on the outlet of the gas bubbler as seen in several of the experiments done.	58
26	Addition of Mg ₂ Si in 10% HCl with oxygen present (left). Addition of 36% HCl in (Mg ₂ Si + H ₂ O) solution (right).	59

List of Tables

1	Material and equipment used during the project.	32
2	ICP-MS instrument parameters	40
3	Complete overview of the experimental plan showing HCl concentration, amount of Mg_2Si and KOH concentration for every experiment.	42
4	Weight of collected residue against original weight of Mg_2Si loaded in each experiment.	52

1 Introduction

1.1 Background and motivation

With a global climate crisis threatening our future way of life, all eyes have been set on the leap to sustainable development that does not compromise the living standards of future generations. In the middle of this crisis lies the need of a shift from carbon industry towards environmentally friendly production methods.

With increasing energy demand and environmental problems, the use of environmentally friendly energy sources is extremely critical. Throughout the 21st century the amount of energy gathered from solar power has increased exponentially making it the fastest growing energy source worldwide for the past 10 years. Looking back at a capacity of 100 GW in 2012, there is very likely that the 1 TW barrier will be broken in 2022. To follow the scenario "Net Zero Emissions by 2050" of the WEO 2020, the capacity would have to be increased to 1840 GW by 2025 and 3929 GW by 2030 making it account for 15.9% of the worldwide energy supply^[8].

Silicon has been a key element in the development of our largest sectors such as energy, technology and materials. The production of silicon today is done through carbothermic reduction of silica in a Submerged Arc Furnace (SAF), this process is a large contributor the CO₂ emissions. The further refinement for use in PV and electronics is done by processes that are both energy intensive and time consuming. Because of silicons strategic role in production of solar cells and as semiconductor in electronics, it is vital that the silicon is produced efficient and climate friendly. About 40% of the energy costs related to the production of solar cells can be related back to the production of the silicon used. This is also one of the strong motivations behind researching new methods for production of high purity silicon with lower energy costs^[9].

It is desired to find new alternatives that can compete with the carbothermic reduction route of producing silicon, a possible competitor is a route through

metallothermic reduction by the use of for instance aluminium or magnesium. A number of studies have been investigating the possibilities of a route from magnesiothermic reduction of silica to elemental silicon applicable in the solar sector. Silane gas produced from the reaction products of magnesiothermic reduction of silica could be deposited as elemental silicon of very high purity. This process could be the foundations of a new production route that reduces the climate footprint drastically.

1.2 Scope of the thesis

In this master's thesis the objective has been set to dive further into the specific reaction between Mg_2Si and HCl to look at reaction products and behaviour of the reaction in a relatively small-scale reactor. The main focus will be to develop a method to capture the silane gas products and to relate this to different reaction parameters. The literature survey in this field reveals a meager amount of modern research done with focus on the acid treatment of magnesium silicide and its reaction products. The use of a small-scale reactor will allow us to perform the experiments in a safe manner, the experiments will contribute to the large field of silicon research and possibly lay the foundations of a new low-energy route for the production of high-purity silicon.

The project is part of a larger study focusing on producing high purity silicon by the means of magnesiothermic reduction of silica followed by silane gas production and finally deposition of solid silicon in for instance a FBR. An overview of the route from quartz to silicon is illustrated in Figure 1.

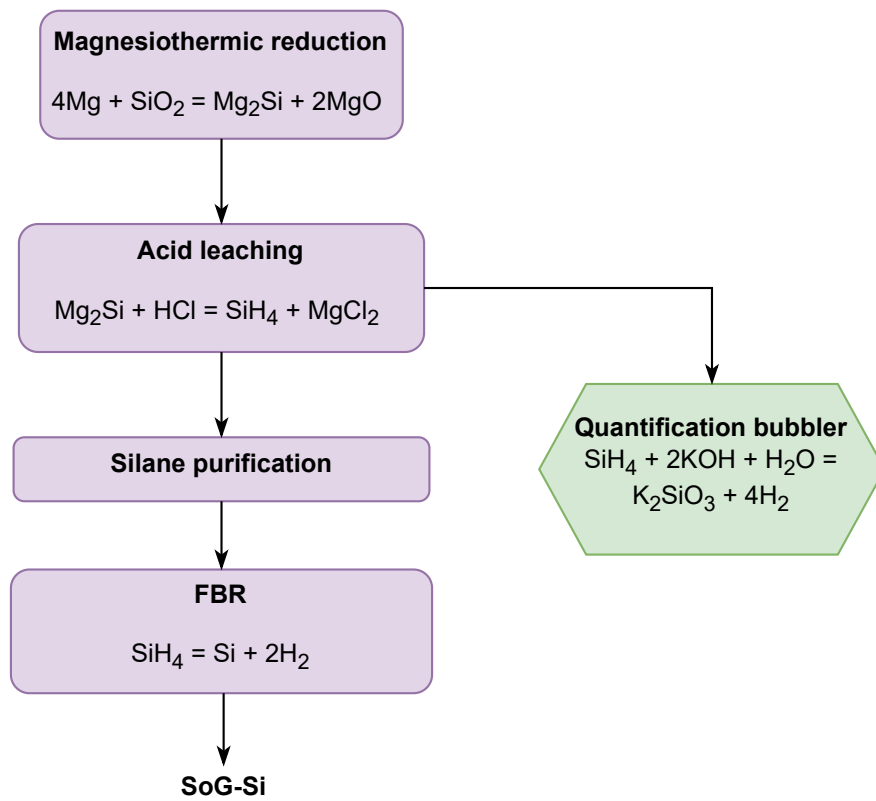


Figure 1: Flow chart of a possible alternative route for producing high purity silicon for solar applications.

2 Theory and Literature study

2.1 Silicon application and production

Silicon is the second most abundant element in the crust of the earth second to oxygen. It is most commonly found in nature as silica and silicates such as quartz or mica. It is recovered from larger deposits of quartzite veins with different qualities. The large abundance of silicon oxides makes it virtually unlimited as a resource although purity and practicality (size, extraction method, etc.) varies considerably among the different quartz types around the earth^[10].

The major areas of use for silicon is as alloying element in steel, cast iron and aluminium, and as oxygen remover in steel alloys. Pure silicon is also used as a backbone in the semiconductor industry both in electronics and in photovoltaic cells as well as in chemical industry in the production of silicones. The broad area of use makes silicon one of the most versatile building blocks used by humans in the 21th century^[10].

The production of silicon at industrial scale is done predominantly by carbothermic reduction in arc furnaces where either metallurgical grade silicon (MG-Si) or ferrosilicon (FeSi) is produced. Norway is one of the world's largest producers of both Si and FeSi with companies such as Elkem, Finnfjord A/S and Wacker. Production of high purity silicon on the scale up to 9N is done through treatment of MG-Si which has a relatively low purity. The upgrading of MG-Si is mainly done through the well established Siemens process developed in the 1950s as well as by the use of Fluidized Bed Reactors (FBR). The chemical processes used for silicon purification both produce a high purity product applicable to photovoltaic and electronic purposes^{[11][12]}.

The solar sector is experiencing increased installations of solar energy and this is one of the reasons for the need of even more high purity silicon in the future. It was seen in 2020, a year suffering from the outbreak of the covid pandemic, that solar was the power generating technology with the highest net installed capacity at 39 % of all new installations. The solar industry

is also experiencing a trend of lower price per MWh of produced power. A comparison of the yearly price development with other power sources can be seen in Figure 2^[1].

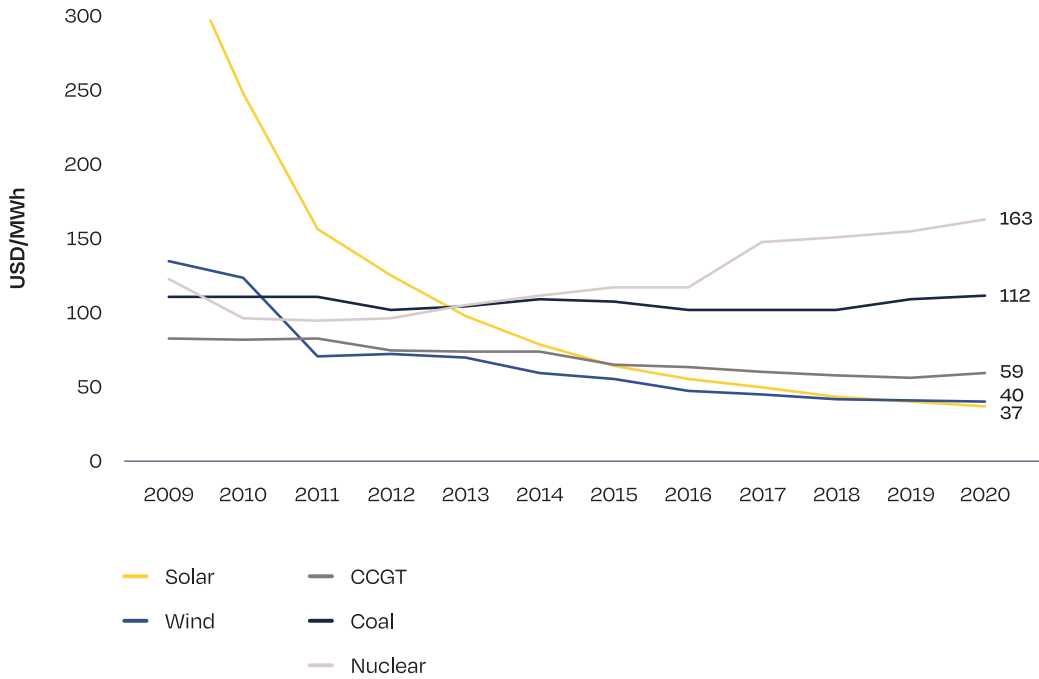


Figure 2: Solar electricity generation cost in comparison with other power sources in the period 2009 - 2020^[1]

Even though the global pandemic raged throughout 2020, the solar sector showed a strong resilience with a growth of 18% representing an installation of 138.2GW. The biggest market is China accounting for over twice the amount of installations compared to the second biggest market being the US. China is also the market with largest grow from 2019 to 2020 with 60% increase as displayed by Figure 3^[1].

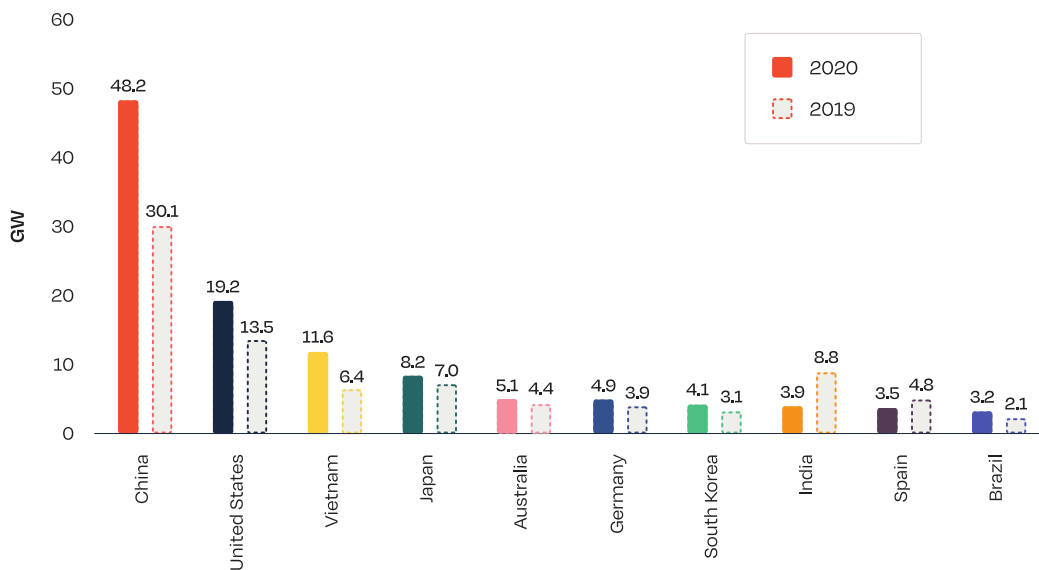


Figure 3: Top 10 solar PV markets in the period 2019-2020^[1]

2.1.1 Global production and areas of application

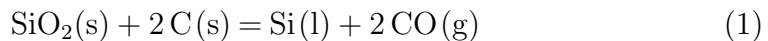
The three biggest producers of silicon (including MG-Si and FeSi) reported in 2019 were China, Russia and Norway producing 5700, 610 and 375 thousand metric tons respectively^[13]. China accounted for approximately 68% of the total production of silicon materials in 2020. The main consumers of FeSi were the steel and the ferrous foundry industry mostly in the Eastern US. The consumption by the steel industry also had a decreasing amount from 2019 to 2020 in line with the global Covid-19 pandemic. For MG-Si metal the largest consumers were the aluminium alloy and chemical industry. The semiconductor and PV industry also consumed a considerable amount of silicon metal^[13].

2.1.2 Carbothermic reduction

The industrial production process for MG-Si is most commonly done through carbothermic reduction of silica in a submerged arc furnace (SAF) with three phase alternating current. A general schematic of the different parts of a silicon plant today can be seen in Figure 4. The furnace has three electrodes

submerged in charge material consisting of quartz, carbon material and in the case of a ferrosilicon furnace also iron raw material such as pellets, sinter or scrap. For the composition of charge material, quartz (SiO_2) is the most common silicon material used while carbon material usually is a mix between coke, coal, charcoal or wood chips. The charge is added on top of the furnace and stoked against the electrodes where the reduction of quartz into silicon takes place due to the heat produced from electric energy. The bottom of the furnace is kept at an operating temperature range of 1900-2000 °C. Silicon is tapped from the bottom of the furnace into ladles where it potentially can undergo further purification through for instance ladle refinement with gas flow of air and oxygen as well as addition of quartz, lime and in some cases cooling metal. The major impurities found in MG-Si are the original trace metals found in the quartz deposit being iron, calcium, aluminium, magnesium, titanium as well as carbon from the other raw materials. The ladle refinement step effectively removes inclusions such as aluminium, calcium and magnesium as well as some of the produced silicon as displayed by the Ellingham diagram seen in Figure 5^{[14][15]}.

The furnace reaction can be simplified as seen by Equation 1 where liquid silicon and gaseous carbon monoxide is produced from the charge materials being quartz and carbon. In reality this process is much more complicated since intermediates such as SiC and SiO also affect the process. The furnace is also often explained by the formation of a hot zone (lower part) and a cold zone (upper part) where different reactions are more present^[16].



Loss of silicon through production of SiO gas from the furnace is one of the dominant factors responsible for reduction in metal yield, this is a reaction that occurs in the hot zone. The full chemical equation can be seen in Equation 2 where SiO production is taken in account, this compound will react with oxygen momentarily producing fine powdered silica (SiO_2) in the cold zone of the furnace. The silica fume is recovered from the exhaust

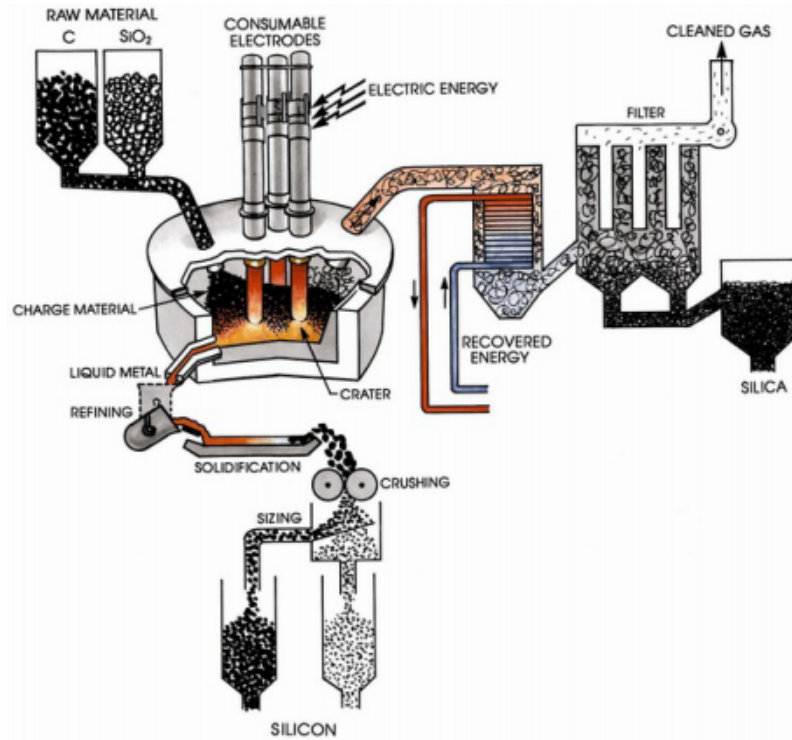
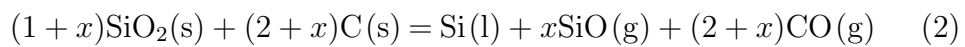
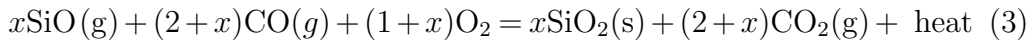


Figure 4: A standard silicon plant showing the process from raw material to final product^[2].

gas from the tap holes and from the furnace top, this product is known as microsilica[®] and has found an area of use as a component in concrete production. Another byproduct in standard silicon plants is the solidified material in each tapping or refining ladle known as skulls. The skulls are CaO–SiO₂–Al₂O₃ based slag removed from the ladle walls which do not meet specifications, they are therefore sold to the silicomanganese-alloy producers for a lower price. A typical yield of silicon in the SAF is in the range 80 - 90%, where losses are mostly in the form SiO gas that is collected as microsilica. Silicon yield is affected by several production factors such as carbon material and stoking.^{[17] [18]}.



The off-gases SiO and CO are released from the furnace where they immediately react with oxygen into SiO₂ and CO₂ respectively, this reaction is also accompanied by the release of heat as seen in Equation 3. The heat production from the off-gases is a big source of energy that can be used further for production of electricity or for district heating.



2.1.3 Production disadvantages and climate aspect

It is clear from the chemical equations that the production of Si via carbothermic reduction has a large production of climate gases such as CO₂ and CO that are released into the atmosphere. Greenhouse gases such as NO_x and CH₄ are found to be produced in the submerged arc furnace as well. The amount of gases is found to be dependent on factors such as furnace type, operation of the furnace and carbon material. Emissions like these are normally sucked into a fume collector before sent out through the chimney, fume hoods are placed over the tap holes and over the furnace top. Gases that have escaped through these fume hoods are called "fugitive" or "diffuse" emissions. Emissions like these may be due to leaks in the collection system or from violent gassing over the fume collectors. All pouring of metal from full ladles will also produce an amount of dust particles that are not collected. Gassing from the tapping holes is especially susceptible to violent gassing when the distance between tapping holes and electrodes are minimal, this is a result of the rotating oven and the electric arc around the electrode tips^[16].

The reduction of silica is producing carbon monoxide gas according to Equation 1. The CO-gas will further oxidise to CO₂ in the furnace top when reacting with oxygen before it flows through the filtering system and leaves through the emission pipes. The combustion of carbon materials from electrodes (pre-baked for MG-Si/Söderberg for FeSi) and furnace charge is also found to produce CH₄. The contribution of greenhouse gases is found to be

highly dependent on^[16]:

- Alloy type: Reducing pure quartz requires a larger amount of energy than reducing iron oxide. The larger the amount of silicon the larger the emissions of greenhouse gas.
- The choice of carbon materials will affect the emission of greenhouse gases.
- Furnace operation and charging method will have a strong influence on NO_X and CH_4 production. Continuously even charging is also found to reduce emissions compared to batch-wise charging.

The nitrogen oxides emissions are dangerous due to their role in creating fine particles and ozone smog in the atmosphere. Other biological problems are acid rain, eutrophication and bronchial suffering. Formation of NO_X -gases can be separated into fuel and thermal NO_X -formation, fuel NO_X is formed from oxidation of N contamination in the solid fuel while thermal NO_X is due to direct oxidation of N_2 in the air at high temperature. This temperature is also found to be dependent on local reactions of SiO combustion at the charge-surface and from tap holes, increasing the temperature and thereby the NO_X -formation^[16].

In addition to the formation of climate gases in the furnace, earlier parts of the value chain are also contributing to further emissions. For instance the production of quartzite that is done through mining and transporting to the plants. The quality as well as the size is also a regard that limits the use of different quartz qualities. To obtain a gas permeability as well as an acceptable electric resistance in the furnace, the quartz has to be charged as lump size quartz raw material (generally 10 –150 mm)^[10]. Using small sized quartz rocks will increase the electric resistance in the furnace as well as lead to a low gas permeability which could cause blow-outs from the gas production. This size restriction is therefore the reason why sand of high quality cannot be used in the furnace^[16].

2.2 Metallothermic reduction

Metallothermic reduction reactions (MRR) are another approach to the reduction of oxides back to their pure elements. The process involves using a reactive metal to reduce oxides through a displacement reaction. A general mechanism can be described by Equation 4 where an element oxide or halide (CL, F, Br or I) (AX) gets reduced by metal B into its elemental state (A) and metal B is oxidised to BX.



Use of this reduction method dates back to 1808 when Humphry Davy isolated alkali metals. Production of aluminium was later done by metallothermic reduction by the use of sodium as the first large scale MRR. Today the metals used in MRR are usually aluminium, calcium, iron, magnesium or intermetallics such as Mg₂Si and FeSi. An example of a widely known metallothermic reaction is the very exothermic thermite reaction between aluminium and rust (Fe₂O₃) that produces molten iron and alumina^[19].

When choosing reducing metal compounds there are several factors that needs to be taken into account along with price and practicality etc. Some factors that make a reduction material suitable for MRR are^[20]:

- Strong affinity to the compound that is to be reduced.
- High boiling point.
- Low vapor pressure.
- Produce a slag that easily can be melted or leached away.

Viable metals that will be discussed further are aluminium and magnesium of which magnesium has been used in this project. Both metals have shown to be alternatives to carbothermic reduction.

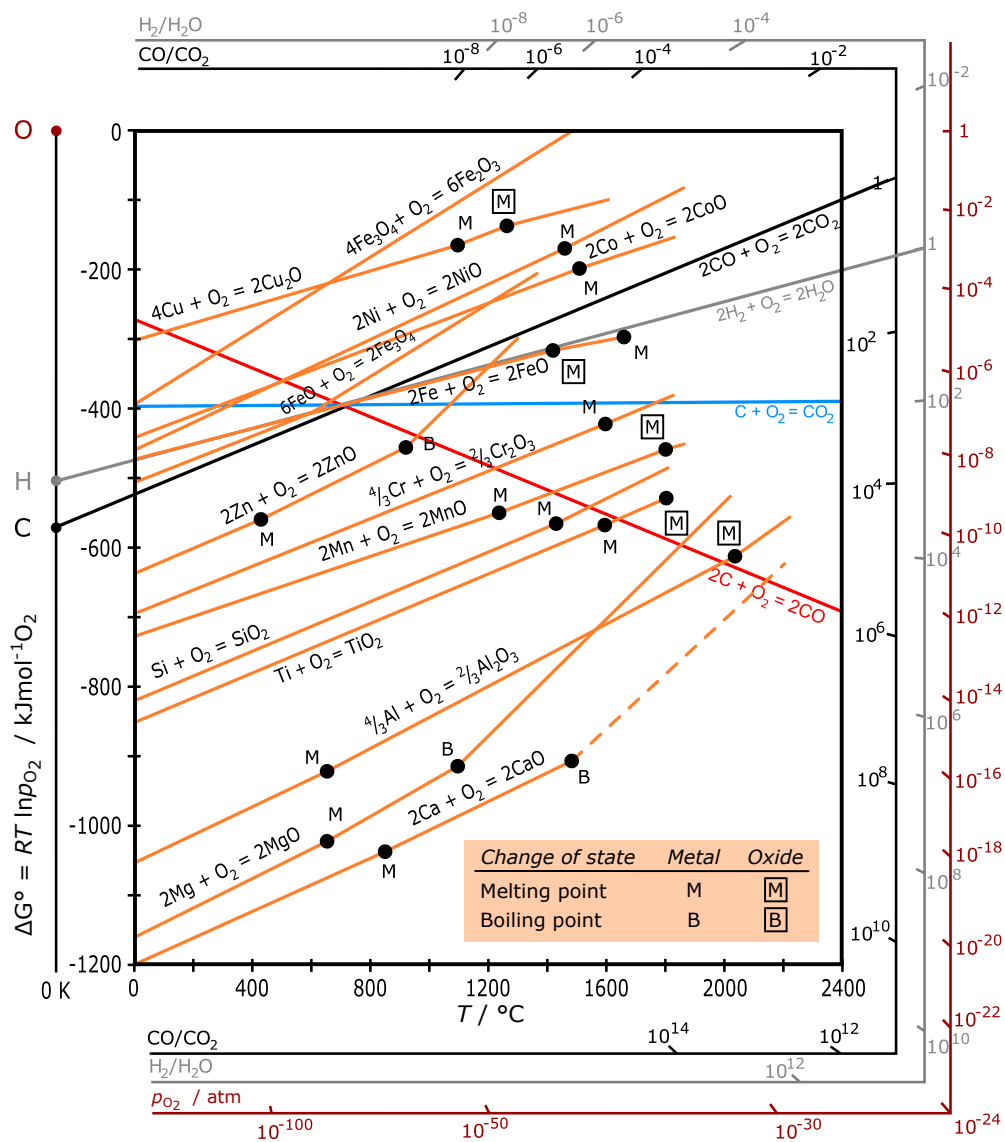


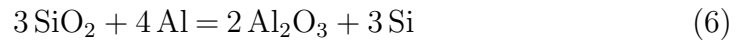
Figure 5: Ellingham diagram showing the stability of various metal oxides^[3].

2.2.1 Aluminothermic reduction and the SisAl process

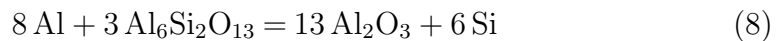
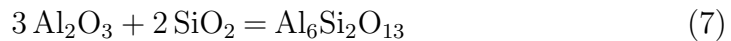
As seen in the Ellingham diagram in Figure 5, aluminium will oxidise according to Equation 5.



Aluminium has shown to be a viable reduction source for the production of silicon from both SiCl_4 and SiO_2 ^[21]. The reduction reaction between silica and aluminium can be described by Equation 6. This reaction is highly exothermic and will produce enough energy to sustain the reaction without need for additional energy input^[22].



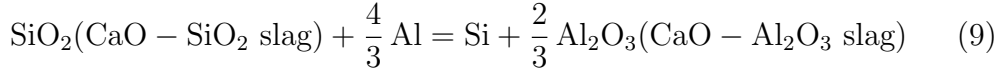
This reaction is applicable for the production of silicon, but has the disadvantage of forming intermetallic oxides such as mullite which can prove hard to remove by acid leaching. The two possible followup reactions are happening as explained by Equation 7 and Equation 8.



As per now the use of aluminium for silicon production is constrained due to practical reasons such as higher cost compared to carbon.

The recent SisAl Pilot Project from Horizon 2020 funded by the EU aims to test the use of aluminothermic reduction as an opponent to carbothermic reduction for silicon production. The suggested production route aims to reduce silica in the form of a CaO-SiO_2 slag by the use of elemental Al collected from secondary sources such as scrap metal or dross. The reaction

products consists of Si metal and a CaO-Al₂O₃ slag as described by Equation 9. The product slag is later separated by hydrometallurgical refining so that the CaO-SiO₂ slag can be used again as reactant.

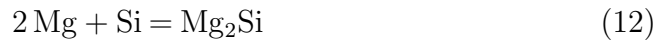


2.2.2 Magnesiothermic reduction

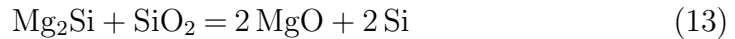
Magnesium has also shown to be a possible reduction material in the process of making elemental silicon from silica. This reaction is complex and linked with the formation of several intermediate compounds. The simple reduction reaction can be explained by Equation 10 where magnesium reduces silica into magnesia and pure silicon^[23].



This reaction is found to produce Mg₂Si in early stages according to Equation 11 or Equation 12 in the case of excess Mg reactant.

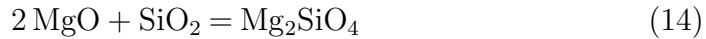


Some silicon is also assumed to be produced through the reduction of silica by Mg₂Si as seen in Equation 13^[22].



Further the formation of the intermediate fosterite is also possible, making the reaction mechanics quite complex. The formation of fosterite is sug-

gested to be caused by the reaction between magnesia and silica according to Equation 14^[23].



The reaction is proceeding at temperatures as low as 500 °C which is substantially lower than that of carbothermic reduction happening in the temperature range around 2000 °C^[24].

The magnesiothermic reduction of silica as large scale production route for MG-Si could be very competitive to carbothermic reduction if the magnesium could be used multiple times. It is seen from the reaction equations that no Mg will leave as product gas in the same way as CO₂ from carbothermic reduction. If the MgO could be used to produce new Mg it would be a renewable reduction material that could be part of a new environmentally friendly silicon production route.

2.3 Upgrading to SoG-Si

The quality of silicon is separated into three main categories. From lowest quality to highest we have metallurgical (MG-Si), solar grade (SoG-Si) and lastly electronic grade (EG-Si). The purity requirements of these are commonly considered to be respectively in the range of 99%, 6N and 9N. The production of high purity silicon is mainly done by treatment of already produced MG-Si. The production of SoG-Si is today done through the Siemens process where MG-Si is upgraded into SoG-Si by a relatively energy consuming refinement route^[12].

The upgrading from MG-Si to SoG-Si is necessary to reduce the amount of impurities to an acceptable level for use in solar cells. Impurities like B and P are desired in small amounts to form p-n junctions for power generation, other impurities like Ti, Ca, Al, etc. are undesirable as they lead to defects and formation of dislocations. Small amounts of impurities can lead to significant reduction in cell efficiency as displayed by Figure 6, it is therefore vital that

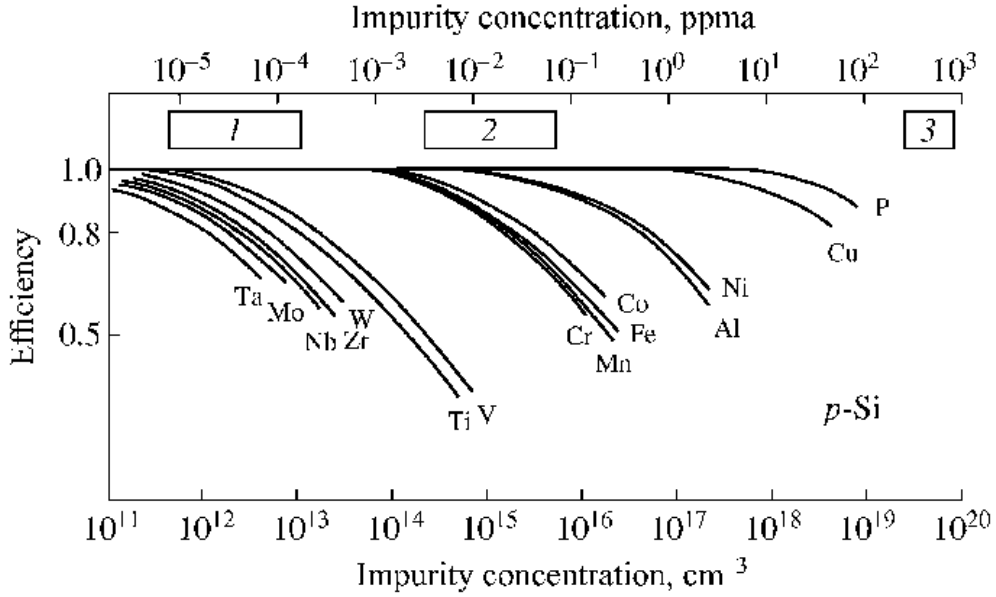


Figure 6: Impurity concentration limits in p-type Si determining the reduction in efficiency of solar cells: (1) EG-Si, (2) SoG-Si and (3) MG-Si^[4].

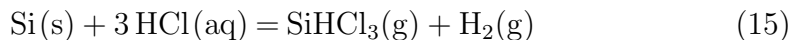
the refinement step is thorough and efficient^[25].

Some impurities can be tolerated in higher levels as they do not have as high effect on the cell efficiency compared to other impurities that may affect the cell performance significantly even in extremely low concentrations. The process of upgrading MG-Si into SoG-Si can be done either by a chemical route or a metallurgical route, the chemical route is the most common method represented by use of the Siemens process and the FBR.

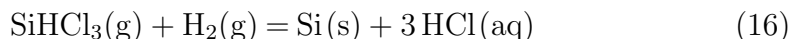
2.3.1 Chemical route: Siemens process

The Siemens process takes MG-Si and converts it to SiHCl_3 before decomposing it back to polycrystalline silicon without transition metal and dopant impurities. This process is considered expensive and slow, but produces a product of extremely high quality that is applicable for both solar and electronic applications. The first part of the process takes the solid particle from MG-Si and converts it into trichlorosilane by the use of hydrochloric acid in

the presence of a catalyst as seen in Equation 15^[25].



The liquid trichlorosilane undergoes a series of distillations until it reaches a purity of EG-Si quality. The silane gas is then reduced by hydrogen in a Siemens reactor where the silane gas is deposited as fine polycrystalline Si particles on Si rods at high temperature ($T > 1100^\circ\text{C}$). The decomposition of trichlorosilane is showed in Equation 16.



The deposition step at the end of the Siemens process is very energy intensive, making the total process very energy demanding. The total polysilicon production process was reported to have an energy consumption of approximately 200 kW h kg^{-1} Si produced in 2009. In 2019 the power consumption was about 85 kW h kg^{-1} Si, when the energy recovery from heat is taken in account the overall power consumption is calculated as $43.75 \text{ kW h kg}^{-1}$ Si. The Siemens process can be seen in Figure 7, where the silicon rods (b) are placed inside of the Siemens reactor (a) and a product of high purity EG-Si is made (c)^{[26] [25]}.

The most critical aspect of the Siemens process is the temperature control needed for efficient silicon deposition on the filament rods while temperature is not exceeding the melting point of the filaments. The deposition rate is also vital in producing a uniform polycrystalline product that can be used for semiconductor and solar applications^[27].

2.3.2 Chemical route: Fluidized Bed Reactor

Opposed to the use of HCl_3Si in a Siemens reactor is the use of the highly volatile monosilane (SiH_4) in FBR. The process of using a FBR has shown to be very advantageous in the production of low-cost high-quality silicon. The FBR is continuous rather than a batch reactor as the Siemens reactor and



Figure 7: (a) Basic Siemens reactor. (b) As grown polysilicon rods after a reactor run. Current generation reactors have many more rods. (c) Final polysilicon chunks^[5].

it has a significantly lower energy consumption per mass silicon produced. Another advantage is the ability to produce more silicon per volume of the reactor.

The FBR uses small seed particles of pure silicon that are fluidized by silane gas from underneath. Decomposition of silicon from the silane gas will cause silicon growth on the seed particles. When sufficient size is reached, new particles are used and so on. The utilization of a FBR enables a continuous production of high purity silicon from silane with greatly reduced energy cost.

Companies like REC and SunEdison have a history of using the FBR in favor of the Siemens process. Wacker has also had research programs focusing on using trichlorosilane (TCS) in FBR. The main advantage of the FBR is the uncomplicated nature of the process as well as the energy demand which is relatively low. The use of TCS in FBRs has shown to be difficult as the reverse reaction has shown to be happening very aggressively reducing the final yield. For silane based reactors the final product has shown to have a undesirable porosity^[28].

To reach a purity of that of EG-Si we need to produce an easily purifiable compound such as trichlorosilane or monosilane which are easily purifiable by methods such as distillation. Trichlorosilane is decomposed afterwards on hot Si-rods in the Siemens process while monosilane is usable in a FBR. The differences between Siemens and FBR is firstly the precursor gases being TCS for the Siemens reactor and SiH_4 and H_2 -gas for the FBR. Use of silane has rather challenging properties making up-scaling difficult if not the proper risks are taken into precaution.

2.4 Silane properties and use in SoG-Si production

Silanes are a group of silicon containing compounds bound to different elements such as halogens (halosilanes), other groups are organosilanes and hydride functional silanes. The simplest form is SiH_4 often known as monosilane, which lays the nomenclaturic basis of all silicon chemistry. The main focus in this project will be the hydride functional silanes such as monosilane, disilane, dichlorosilane, trichlorosilane and so on. Of all the thousand variants of hydride functional silanes available, only a few of them are of any commercial interest such as inorganic and organic silanes as well as polymeric siloxanes. These few compounds represent a broad range of application such as manufacturing of EG-Si, epitaxial Si-deposition, as selective reducing agents and as reaction intermediates used for production of other silanes or silicones^[29].

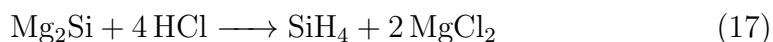
The commercial interest for silane gases began in the 1960s when the semiconductor market was at its development phase. Though this is still the main market using silane gas there has also been found other uses as described above. Of all the silanes associated with production of silicon metal of high purity, trichlorosilane is the most preponderant and the only inorganic silicon hydride produced in large scale. It is both used as an intermediate when producing other silanes as well as the main compound used when producing high purity silicon in large scale. This study will be focusing mainly on the formation of binary silanes such as SiH_4 , Si_2H_6 and higher. Understanding both chemical and physical properties of these compounds becomes

vital when using them in groundbreaking modern technologies that are both robust and safe.

2.4.1 SiH₄

Monosilane is an inorganic compound composed of silicon bonded with four hydrogen atoms. Silicon is in the same elemental group as carbon, and SiH₄ can be seen as the silicon analogue of CH₄, having a much higher reactivity with transition metals. SiH₄ is also known to be highly pyrophoric, combusting spontaneously in air without the need of an ignition source. Compared to higher order binary silanes, monosilane is the most thermally stable with decomposition at 500 °C, disilane and trisilane are known to be much less stable. When used in the Siemens process with the presence of hydrogen, silane has been found to decompose at temperatures as low as 640 °C, the product is a thin film of deposited silicon metal consisting of amorphous hydrogenated silicon^[29].

There are several chemical routes used to produce monosilane gas, a common way is by reacting a strong acid with magnesium silicide. This reaction is extremely reactive in acid and if conducted in oxygenated atmosphere the produced silane gas will ignite momentarily. The reaction is shown in Equation 17 where hydrochloric acid reacts with magnesium silicide forming magnesium chloride and silane gas. The gas is very important as a precursor to produce elemental silicon with high purity grade through chemical vapor deposition. This is due to the fact that silane decomposes above 420 °C into elemental silicon and hydrogen gas^{[29] [30]}.



This reaction procedure is associated with a relatively low yield as well as accompaniment with higher order silanes which leads to purification difficulties later on. Exclusive production of monosilane can be done through the hydrolyzing reaction with ammonium chloride or ammonium bromide in anhydrous ammonia at room temperature^[30].

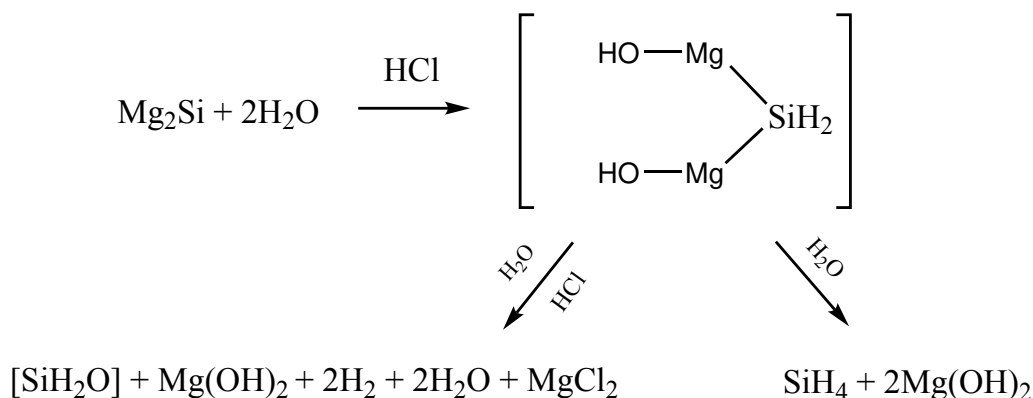
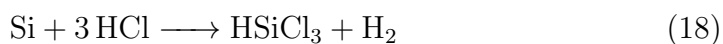


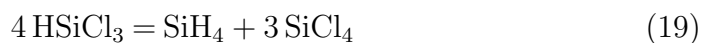
Figure 8: Mechanism of acidic hydrolysis of Mg_2Si into monosilane.

The mechanism of the reaction between Mg_2Si and HCl is suggested to happen according to Figure 8 where a dihydroxymagnesiumsilane intermediate is formed before the separation into two reaction paths. The first path involves the further reaction with water into MgCl_2 , SiH_2O , etc. Another possible reaction product is $\text{Mg}(\text{OH})_2$ which has very low solubility in water compared to MgCl_2 . From the thermodynamical calculations in Figure 9 done with HSC it can be seen that both ΔG_{rx} and ΔH_{rx} are negative for all practical temperature values. This gives the information about a spontaneous and exothermic reaction^[29].

Another method is done by reacting metallurgical silicon with hydrochloric acid to form trichlorosilane and hydrogen gas.



The redistribution into monosilane and tetrachlorosilane can further be done by the use of a catalyst.



Silane is known to be a pyrophoric gas making it capable of ignition below 54 °C. Leaked silane gas in air is highly ignitable, when diluted in inert gases

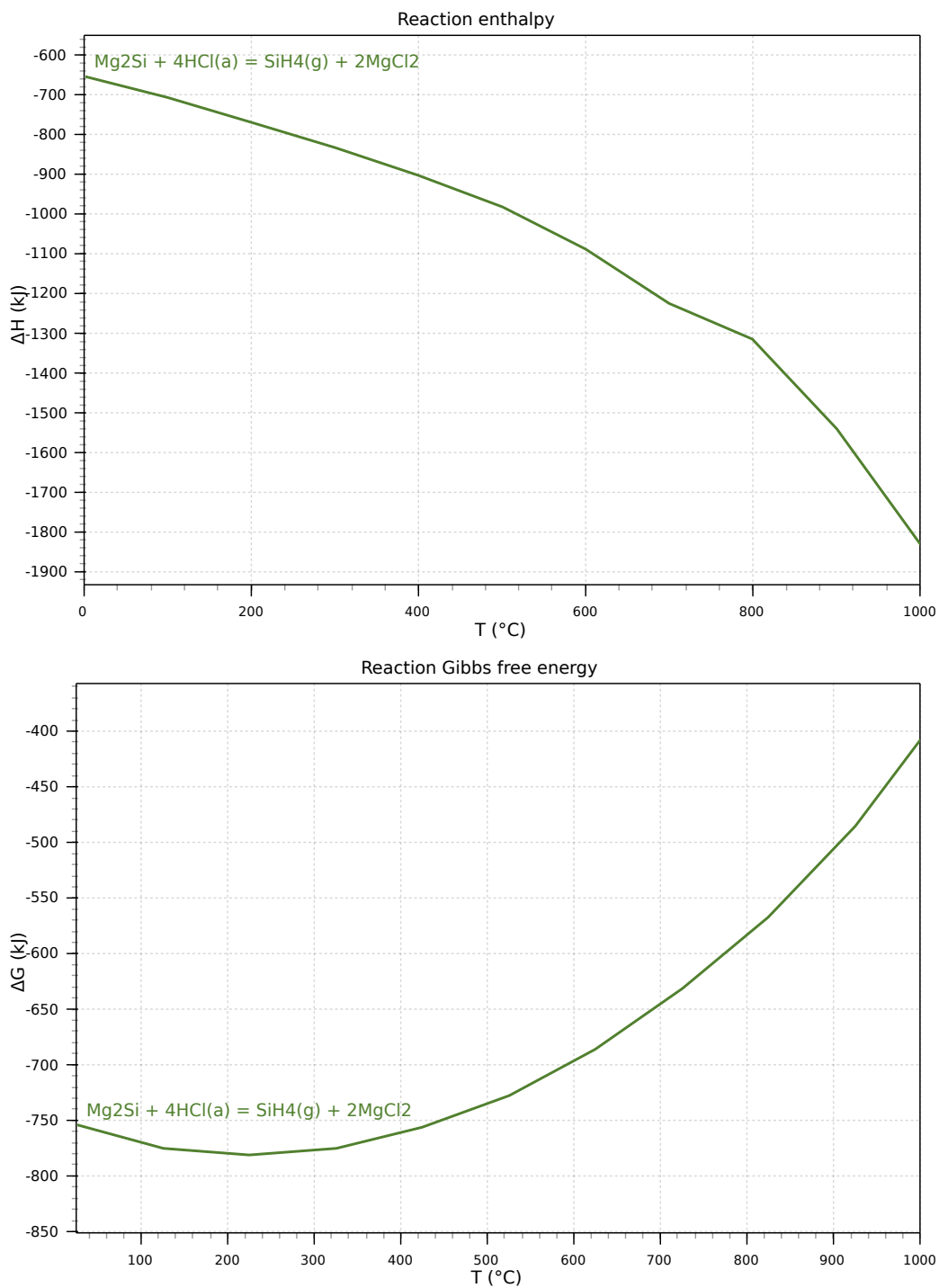
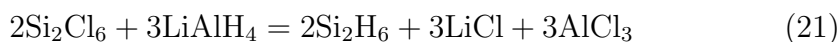


Figure 9: Graphs showing the simulated enthalpy and Gibbs energy curves for the reaction between Mg_2Si and HCl .

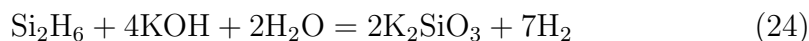
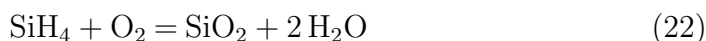
such as nitrogen or argon, ignition is even more likely when exposed to open air compared to pure silane gas.

Production of silane from silicon halides is usually the most convenient way at laboratory scale. This reaction can be done with SiCl_4 and lithium aluminium hydride in diethyl ether according to Equation 20 and Equation 21^[30].



2.4.2 Oxidation of SiH_4

All of the silicon hydrides are oxidised easily, for instance when oxidised in air it will form the reaction product water and white silicon dioxide by the reaction described in Equation 22. Silanes do not have a strong reaction with water or weakly acidified solutions. It will on the other hand have a rapid reaction in basic solutions where it decomposes into hydrogen gas and dissolved silicon. An example can be seen in the reaction with KOH ^[29]:



Complete hydrolysis in basic solution could be used to do quantitative measurements of silane production either by measurement of produced hydrogen or by analysis of silicon in the basic solution. For Equation 23 it is clear that four hydrogen molecules are liberated for each Si-H bond and that one silicon atom is present in the solution as K_2SiO_3 . The downside of doing quantitative analysis of either hydrogen or silicon is that there is no way to

tell the difference between the original silane gas as seen in Equation 23 and Equation 24. On the other hand this is a method of analysis that is primitive and very easy to apply to a silane gas flow. Other methods of hydrolysis are the reaction with methanol at room temperature to produce several methoxy-monosilanes. This reaction is catalyzed by metallic copper^[29].

2.5 Literature survey

In this section a presentation will be given of studies involving silane gas production and behaviour. The main interest will be the literature done on the specific reaction between Mg_2Si and HCl which is most similar to the experiments done in this project.

Alfred Stock (1933) first investigated the reaction between Mg_2Si and HCl , and the different silicon-containing gas products. It was reported a yield of 23% silicon present in silane gases compared to the original silicon present in Mg_2Si . The composition was found to be approximately 40% monosilane, 30% disilane, 15% trisilane, 10% tetrasilane and 7% higher silanes. The experiments were carried through by dropping magnesium silicide - formed through reduction of silica by metallic magnesium - onto a solution of hydrochloric acid^[31].

Johnson and Isenberg (1935) built on the discoveries done by Stock and introduced ammonium bromide in liquid ammonia to reduce Mg_2Si . By avoiding aqueous solutions such as HCl a yield of 70 - 80% silicon was achieved which is substantially higher than that achieved with HCl systems done by other authors. The high amount of yield was achieved at experimental temperatures of -33°C , reducing the temperature further down to -80°C resulted in a big reduction in yield to less than 20 %. It was also reported that for the low-yield experiments, the amount of hydrogen was 4 to 5 times as great in volume compared to that of silane while the magnitude was of the same order for that of the high-yield experiments. The amounts of magnesium silicide used in the experiments was rather large, going from 2 g up to as much as 137.3 g^[32].

Nandi et. al. (1993) produced silane gas from Mg_2Si reacted with HCl of various strength. The study investigated this reaction with main focus on silane yield against reaction temperature, Mg_2Si particle size and % by volume strength of the HCl. Gas chromatography analysis pointed towards formation of mostly monosilane (SiH_4), but also disilane (Si_2H_6) formation. There was no indication of formation of higher order silanes in this project, this could be a result of decomposition of higher order silanes at the relative high temperature.

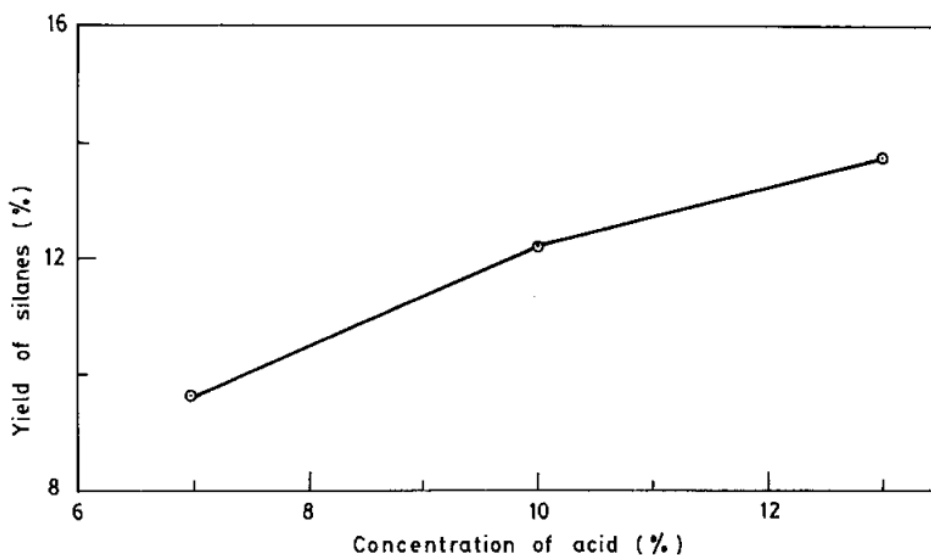


Figure 10: Relationship between silicon yield in the form of silane gas at different HCl concentrations (v/v%)^[6].

For the experiments with increasing HCl concentration at 23 °C, a trend of increased silane production was observed. This trend can be observed in Figure 10, where 7%, 10% and 13% HCl was used. The increase in silane gas is explained by a lower amount of water available for the produced silane gases to react with. The GC setup used in this project could not be used for experiments with larger concentrations of HCl as large amounts of acid vapor could not be removed easily. Low concentrations of acid resulted in a very slow reaction together with a low silane yield, optimal reaction condition was

therefore decided to be with 10% HCl.

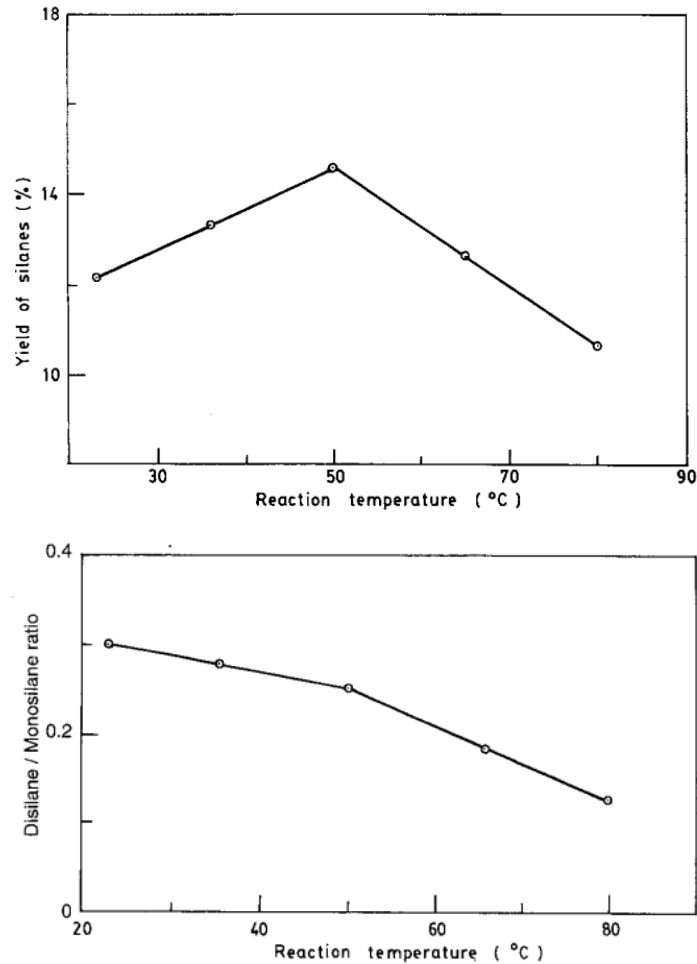


Figure 11: Relationship between silicon yield and silane ratio against increase in reaction temperature (°C)^[6].

Figure 11 shows the experiments done at increased temperatures (23, 35, 50, 65 and 80 °C) with 10% HCl. The plots display a clear increase in silane yield until about 50 °C before decreasing with further temperature increase. The same experiments show a strong decrease in Disilane/Monosilane ratio for increased temperatures, disilane was therefore proven to be promoted at lower reaction temperatures with $\text{Si}_2\text{H}_6/\text{SiH}_4 \approx 0.3$ at room temperature.

Nandi et al. lastly investigated the Mg_2Si particle size effect on silane pro-

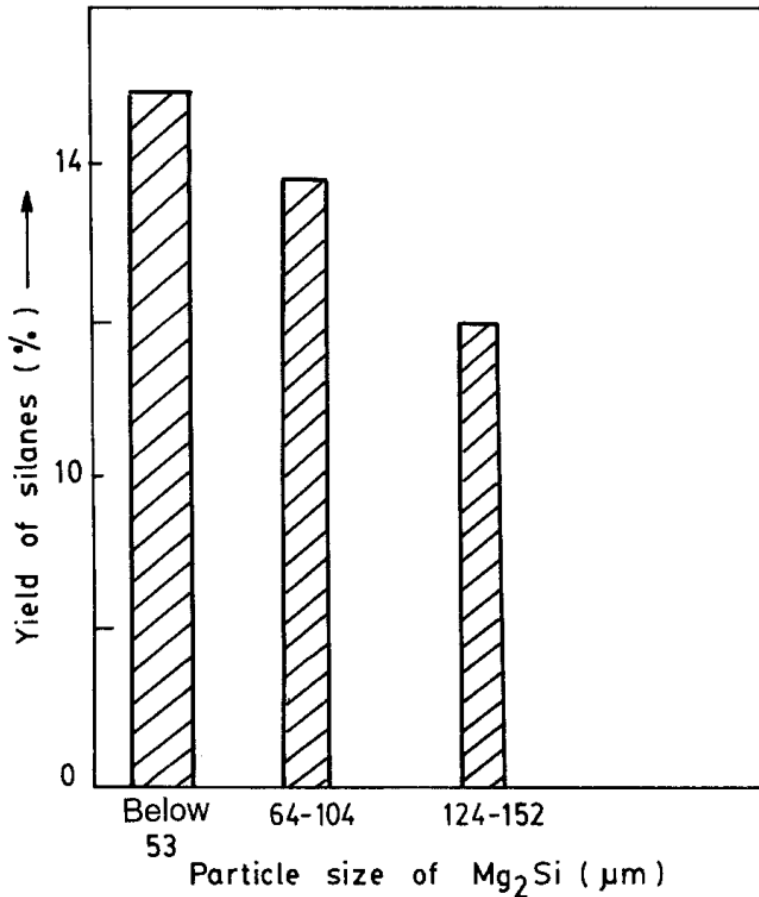


Figure 12: Caption

duction. The results shown in Figure 12 show a trend towards increased silane production for smaller Mg₂Si particles. This result is explained by the reaction mechanics where smaller particles have a larger surface area open for reaction with acid. The maximum yield from the experiments were approximately 15 % silicon captured as gas compared to the original amount found in magnesium silicide.

The experiments done by Nandi et al. from 1993 is the public literature most comparable to the study done in this thesis. The Mg₂Si was prepared from rice husks and the paper concluded that this process was applicable for deposition of Si films in the PV industry. The specific reaction between Mg₂Si

and HCl has not been investigated much since the turn of the millenium, the research done by Nandi et al. dates back 29 years and there is still much to reveal in the field of silane chemistry, both in a production aspect and in the field of post-production treatment for commercial use.

Tan et al. (2019) investigated the hydrogen generating reaction between Mg_2Si and two strong reducing agents being NH_4Cl and NH_4F . The reaction was investigated with the intent of finding the conditions promoting hydrogen production rather than silane. Reaction with NH_4Cl had immediate silane formation indicated by sparks at reaction start together with formation of white dust. The use of NH_4F suppressed the formation of silane very effectively having no observable sparks or dust. Figure 13 shows the measured gas formation during the reaction between Mg_2Si and NH_4F , it is seen that a small amount of monosilane is produced at the start, but that the hydrogen formation is dominating. The formation of SiH_4 was in this setup quantified by the use of a 30 wt% NaOH solution that reacted according to Equation 25.



The amount of reaction gas being silane from volume change calculations was found to be 1.47% and 0.38% for the use of NH_4Cl and NH_4F respectively. This method utilises the volume expansion when silane reacts to hydrogen gas in NaOH and increases the volume by a factor of 3. There was also done milling treatment of the Mg_2Si particles by the use of a ball mill for 2h and 5h, this showed great increase in the reactivity of Mg_2Si and higher production of H_2 ^[7].

Schwarz et al. (1922) investigated the reaction mechanics of Mg_2Si reacting in aqueous HCl. The reaction was hypothesized to occur in several steps, the first in which the intermediate hydrolysis product (dihydroxymagnesiumsilane) is made according to Figure 8 followed by the formation of silane gas from the violent reaction resulting from the breakage of the Si-Mg bonds. An opposing reaction suggested was one which suppresses the formation of silane in favor of formation of H_2 . The total reaction is seen affected both

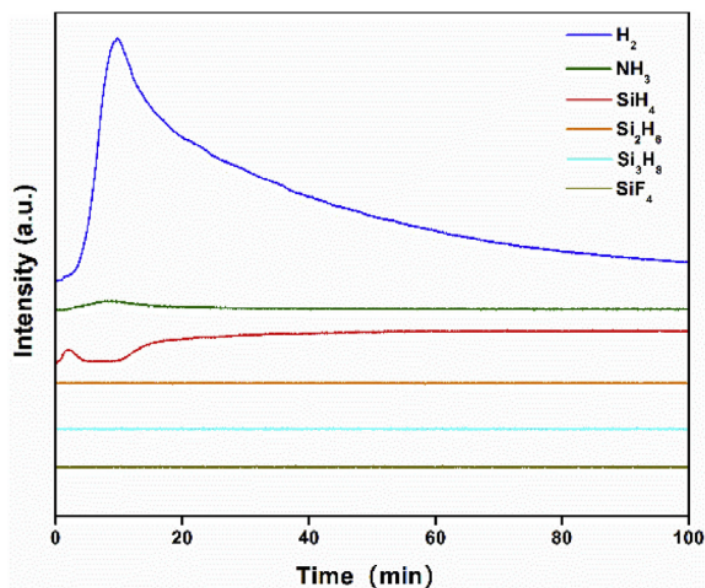


Figure 13: Gas characterization of the reaction between Mg_2Si and NH_4F by mass spectrometry^[7].

by hydrolysis and the reactivity with HCl, the primary reaction is seen dependent on the amount of H_2O available, stronger concentrations of HCl will decrease this availability of water. To low concentrations of HCl will on the other hand suppress the following reactions resulting in lower efficiency. Most authors have concluded in that the use of 10% (w/w) is the most optimal concentration for production of silane gas^{[33] [34]}.

Frank et. al. (1984) did a study involving the silane producing reaction between CH_3Cl and several silicon containing surfaces. The reaction was done in a batch reactor at atmospheric pressure in the temperature range 520-620 K. The main gas products where found to be HSiCl and CH_3HSiCl . For three surfaces being Cu_3Si , Cu_3Si containing 0.4% Zn and lastly pure silicon, the pure silicon was found to produce the largest amount of silane gas product. The copper alloys where however found to increase the selectivity of $(\text{CH}_3)\text{SiCl}_2$ to 85% for Cu_3Si and 95% for Cu_3Si containing zinc. The formation rate of different silanes was calculated to be approximately $2 \cdot 10^{14}$ atoms/cm² · s at 570 K^[35].

Wyller et. al. (2019) investigated the pyrolysis of monosilane (0-100%) diluted in hydrogen at the temperature range 450-530 °C. The study focused on developing a gas analysis setup that allowed for absolute quantification of the different types of silane gases (mono-, di- and trisilane as well as higher order silanes) by the use of a GC-MS. Gas analysis by gas chromatography and mass spectroscopy revealed content of mono-, di- and trisilane as well as silanes with up to eight silicon atoms. The setup was able to differentiate between silanes with up to five silicon atoms, the mass spectra of six higher order silane isomers were also published, something that had not been included in previous literature. The study also found a correlation between formation of cyclic silanes and fines formation during the monosilane pyrolysis. It is therefore hypothesized that avoiding these cyclic silanes can be advantageous in FBRs where fines promote clogging and production difficulties. The main trends found were that the concentration of higher order cyclic silanes increased with increasing temperature and monosilane inlet concentration, the most favorable conditions are therefore found to be low temperature system combined with high monosilane concentration to avoid heterogeneously nucleation^[36].

The autoignition characteristics of silane released into air was studied by Chen et. al. It was found that ignition always takes place in a defined air/silane mixture known as the most reactive mixture fraction. The most dominating factor was found to be the flow velocity, having a sufficiently low flow velocity caused immediate ignition. It was also proposed that both water content and combustion particle products such as silica (SiO_2) could affect the ignition mechanics^[37].

To conclude the literature review, specific literature on the acid treatment of Mg_2Si by HCl has been very limited. There is a great motivation to work with this field in the sense that this production route of silane gas is still much uninvestigated and that there still is much to discover in terms of reaction mechanics. On the other hand there is also a great challenge in doing research involving silane as this adds a HSE aspect in the experimental part. Gas leakage is often related to explosions and health risks and this is often

the cause of the great unappeal when doing research involving silane. In this thesis a small-scale experiment involving silane production will be conducted in a closed reactor at NTNU, Trondheim, with the intent to develop a safe reaction setup and promote work with silane in the future.

3 Experimental procedure

This section will present the experimental procedure that was carried out in the course of this project. As a main focus of the thesis was to develop a new method for silane quantification, the experimental method and design will also be introduced.

3.1 Material

Table 1: Material and equipment used during the project.

Material	Description	Supplier
Ar(g)	5N purity	Sigma Aldrich
HCl(aq)	37% w/w	Sigma Aldrich
Mg ₂ Si(s)	99.5% purity	Thermo Scientific
KOH(s)	85% min (KOH basis), 99.98% (metal basis)	Thermo Scientific
HNO ₃ (aq)	65% w/w	Thermo Scientific
H ₂ O(l)	Milli-Q [®]	Merck
Glass equipment	Used as reaction container	NTNU
Steel and plastic tubing	$\frac{1}{4}$ " diameter	NTNU
Steel connections	$\frac{1}{4}$ " diameter Swagelok [®]	Swagelok
Mass flow controller	1SLPM, Display	Alicat Scientific

3.2 Experimental design

As there were no previously conducted experiments of this sort, a brand new reactor setup had to be designed and set up based on theoretical calculations. It was found that a glass reactor would be suitable for a small scale experiment like this, and it was designed so that Mg₂Si could be pre-loaded into the reactor followed by dropping acid from a dropping funnel also made out of glass. It was extremely important that the entirety of the reactor was air tight, swagelok stainless steel fittings were therefore used for connections between the gas tubing, ensuring no leaks between connected parts of the setup. Connection between the glass parts in the instrument were spherical shaped and lubricated with vacuum grease before being tightened with steel

clams.

Quantification of gas products is normally done through mass spectrometry and/or gas chromatography, but as these methods of analysis were unavailable at the time of the experiments a new method had to be developed. The experimental setup and analysis was based on the strong reactivity of silane gases presented in subsection 2.4.2. A setup was therefore developed so that all the produced silane gas could be measured indirectly as ions in a solution. This was achieved by leading all the reaction gases through a gas bubbler filled with a reactive solution of KOH. Since the solution of KOH could be collected and analysed later by ICP-MS, the use of advanced on-line gas analysis equipment was effectively avoided in favor of offline liquid analysis.

The silane producing reaction between Mg_2Si and HCl was carried out in an Erlenmeyer flask connected to a dropping funnel, both made out of glass. It was made so that the acid could be dropped upon pre-loaded Mg_2Si powder in the Erlenmeyer flask with gas flow leading the produced gases into a gas bubbler that oxidised all product gases into dissolved ions. As a cause of the strong reactivity and self igniting properties of silane in air, argon gas of 5N purity was used to purge the reactor so that no oxygen was present. A mass flow controller (MFC) was used to control the flow rate of Ar gas entering the reactor.

3.3 Procedure

The experimental procedure has been carried through with the goal of investigating the reaction between magnesium silicide (Mg_2Si) in powder form and defined concentrations of hydrochloric acid (HCl). The complications with quantitative analysis of the gas products have been solved by leading the reaction gas through a gas bubbler filled with various concentrations of potassium hydroxide (KOH). The KOH solutions have thereafter been analysed using ICP-MS at the department of chemistry, NTNU, Trondheim.

All experiments have been conducted in glass containers made by the NTNU

glassblowing workshop, the equipment consisted of an Erlenmeyer flask and a dropping funnel for containing reactants as well as glass adapters to the rest of the metal tubing for gas flow. Total volume of the Erlenmeyer flask was approximately 1.5 L and inlet and outlet was of spherical glass coupling covered with vacuum grease. The dropping funnel was designed so that there was no pressure difference in the reactor setup and so that gas flow through the reactor was possible without dropping HCl. The volume of the dropping funnel was approximately 500 mL. Both connection from glass to steel tubing were made as glass/ $\frac{1}{4}$ " swagelok adapters. A sketch of the reaction setup can be seen in Figure 14.

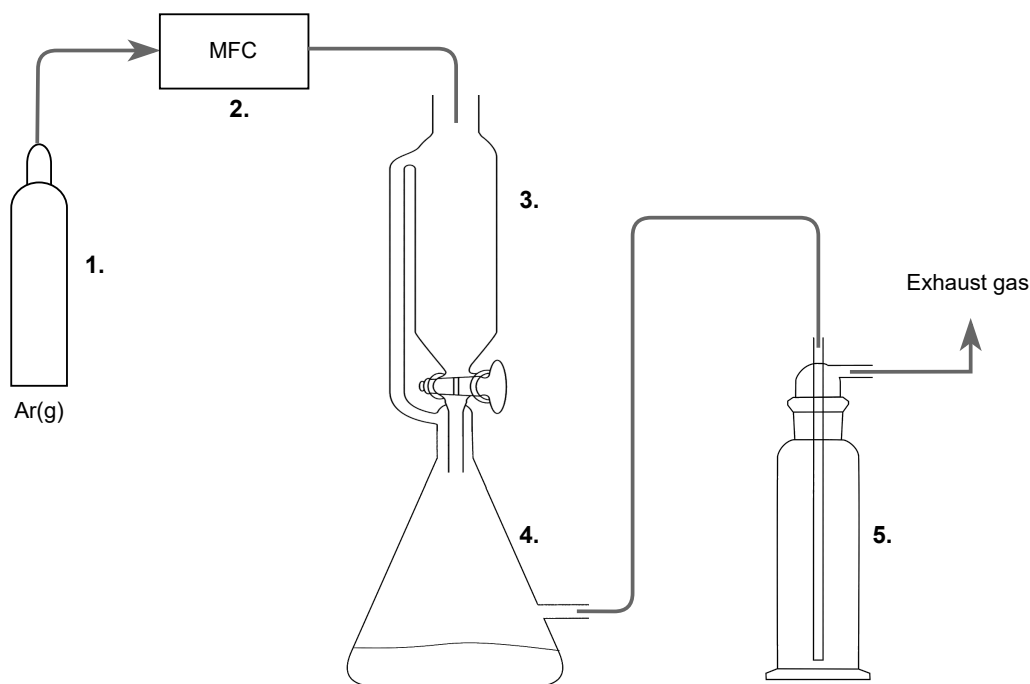


Figure 14: Flowsheet showing the reaction setup used in the experiments. (1.) Argon bottle 99.999%, (2.) Alicat mass flow controller, (3.) Glass dropping funnel, (4.) Glass Erlenmeyer flask (inlet/outlet) and (5.) Glass gas bubbler.

The reactive nature of the product gases has led to the use of inert argon atmosphere for all experiments done. The reactor has been thoroughly purged with Ar-gas with exact flow rates and time spans before the initiation of all

reactions done in this project. The flow rate has been controlled through the use of a MFC (MC-series, 1SLPM) delivered by Alicat Scientific. Through the use of Swagelok[®] adapters all tubing has been sealed properly between all parts in the experimental setup. All tubing was 1/4" and made of mainly stainless steel, the tubing between the argon bottle and the MFC (1. - 2. Figure 14) was made out of plastic. The three last parts being dropping funnel, Erlenmeyer flask and gas bubbler were all supplied from the NTNU glassblowing workshop along with adapters from glass to the steel tubing.

All experiments were conducted with the reactants being solid Mg₂Si powder and aqueous HCl. The Mg₂Si powder and a stirring magnet was always inserted to the open Erlenmeyer flask before attaching the dropping funnel. The dropping funnel was then attached and filled with 100 mL of HCl before tightening the connections with metal clamps. Lastly the gas bubbler was filled with 200 mL of KOH before gas purging was started. All connections were then inspected with leak detection spray and found to be completely sealed.

The solutions of HCl and KOH were prepared from a concentrated HCl solution and KOH pellets respectively. The HCl solution was prepared by diluting the concentrated acid down to desired weight percentage by adding distilled water. The solutions of KOH were prepared by dissolving solid KOH pellets in distilled water to achieve desired molarity.

The storage of Mg₂Si was always done inside a glove box filled with Argon to prevent all oxidation to the reactant powder used in all experiments. Using fine powdered Mg₂Si is always related to problems with oxidation when exposed to oxygen, all samples were therefore taken out one at a time from the glove box inside a small glass sample jar when transported to the reaction setup. All amounts of powder were scaled on a weight scale inside the glove box, this amount was afterwards corrected for by noting down the difference of the weight of the glass jar with powder against the weight when powder had been added to the reactor. All potential contact between Mg₂Si and O₂ was from the moment the glass jar was opened to add powder to the reactor,

until the reactor had been purged with Ar to remove all air.

The following experiments were done by the use of the setup described (see Figure 14), with varied parameters being amount of Mg_2Si , KOH concentration, HCl concentration and the size of the bubbles in the gas bubbler. When referenced in the future, the amount of Mg_2Si corresponds to the initial amount loaded into the reactor (4.) before reaction start. The HCl solution relates back to the solution loaded into the dropping funnel (3.) and the KOH solution is that loaded into the gas bubbler (5.). The temperature of the experiments was neither controlled nor measured during the time course of the experiments, all experiments were assumed to take place at room temperature at approximately 25 °C.

3.3.1 KOH concentration

A trial experiment was done where 200 mg of Mg_2Si was reacted with 10% HCl, the product gases were then bubbled through a 200 mL solution of 0.09 mol L^{-1} KOH for approximately 45 min. The resulting solutions of mainly HCl and KOH were then analysed for Mg and Si by ICP-MS at Department of Chemistry, NTNU.

The concentration of KOH was further varied in six experiments with molar concentrations ranging from 0.1 - 4 mol L^{-1} . This was done to get an impression of the silane decomposition in increasing concentrations of KOH to determine the reliability of this setup. With constant amounts of 300 mg Mg_2Si reacted with 100 mL HCl (10% w/w), the product gas was bubbled through 200 mL KOH with concentrations 0.1, 0.5, 1, 1.5, 2, 3 and 4 mol L^{-1} . All material was then collected from the reactor, HCl and precipitate was collected from the Erlenmeyer flask and KOH was collected from the gas bubbler. This resulted in two samples from each experiment where only the KOH solution was analysed by ICP-MS.

Analysis of each sample was done together with a corresponding blank sample which had undergone identical reaction procedure except for the mixing of Mg_2Si and HCl. All samples were thereafter diluted with water and HNO_3

(65 % w/w) to concentrations acceptable for the ICP-MS instrument. The concentration limits of the elements K, Si and Mg were at a lower limit of 20 ppb and a higher limit of 25 000 ppb for the ICP-MS used for analysis of the reaction products.

The following experimental procedure was used for the first parallel, some adjustments were done for the rest of the experiments. When the reactor setup had been loaded with Mg_2Si , HCl and KOH, a gas flow of argon was set to 0.6 sL/min for approximately 45 min. After purging the reactor with argon, the HCl was dropped upon the Mg_2Si powder with stirring, the gas flow was also lowered to 0.2 sL/min. The reaction was kept going for 20 min before the experiment was terminated and samples were collected in plastic bottles.

3.3.2 Bubbler porosity

The initial experiments with varied KOH-concentrations were repeated again with a porous bubbler with the intent of reducing the bubble size. Comparison of the bubblers used in subsection 3.3.1 and for the rest of the experiments can be seen in Figure 15.

For the following parallels done with the new bubbler, a new procedure was performed in hopes of collecting more silane gas. When the reactor setup had been loaded with Mg_2Si , HCl and KOH, a gas flow of argon was set to 0.6 sL/min for approximately 45 min. After purging the reactor with argon, the gas flow was reduced to 0.01 sL/min before the HCl was dropped upon the Mg_2Si powder with stirring. The reaction was kept going for 20 minutes before the gas flow was turned up to 0.2 sL/min for 10 minutes. After the last gas purging the experiment was terminated and the reactor was disassembled so that samples could be collected.

3.3.3 Amount of Mg_2Si

The third parameter change was done by increasing the amount of Mg_2Si while the other parameters were held constant. The amount of Mg_2Si reac-



Figure 15: Comparison between porous bubbler "level 0" (left) and standard bubbler (right).

tion material was varied from 300 to 600 mg. With constant HCl and KOH concentrations of 10 % and 2 mol L^{-1} respectively, the experiments were performed with Mg_2Si quantities being 300, 400, 500 and 600 mg. Experiments were then performed as before followed by analysis of the KOH solution by ICP-MS. The porous bubbler was also used for all remaining experiments.

3.3.4 HCl concentration

The last parallel of experiments was done with varied strength of the hydrochloric acid. The HCl concentrations were varied from 7.5 to 15 % (w/w) while the concentration of KOH and amount of Mg_2Si were held at 2 mol L^{-1} and 300 mg respectively. The HCl concentrations were increased in the increments 7.5, 10, 12.5 and 15%.

3.3.5 Precipitate

The HCl solutions were at the end of all experiments filtered by the use of a vacuum pump and filter paper. The filter paper was dried in a heating oven at 60°C over the weekend and the amount of precipitate was calculated for all experiments based on the difference in weight between empty filter paper and dried filter paper with solid residue. The dried powder was thereafter collected in sample bags and some selected samples were ground with a pestle and mortar and analysed by XRD and SEM. The sample prepared for SEM was carefully cast in epoxy and polished by the use of SiC paper. The collected samples of precipitate were originating from experiment number 14 and 17, with experimental parameters found in Table 3.

3.4 Characterisation

XRD and ICP-MS was used for analysis of the HCl precipitate and KOH solution respectively. The precipitate from the HCl solutions was additionally analysed by SEM.

The KOH solutions were analysed for K and Si using 8800 Triple Quadrupole inductive coupled plasma mass spectrometry (ICP-MS) system (Agilent,

USA) equipped with prepFAST M5 autosampler (ESI, USA). Each sample was diluted externally by the author using multi-pipette and during the analysis using prepFAST M5 autosampler. Analytes were measured in O2 mode of the system to remove potential interferences. The system parameters during analysis can be seen in Table 2

Table 2: ICP-MS instrument parameters

General parameters	
RF Power	1600 W
Nebulizer Gas	0.78 L/min
Makeup Gas	0.40 L/min
Sample depth	8.0 mm
O₂ mode	
O2 gas flow	0.675 L/min

The collected residue from some of the HCl solutions was analysed by the use of a Bruker D8 Focus powder diffraction system at NTNU. The XRD analysis was done for 2θ values ranging from 10 to 90.4964 with step size 0.02587 resulting in a total analysis time of approximately 83 min. All samples were analysed with a 0.6 mm divergence slit and $\text{CuK}\alpha$ radiation. The SEM used for analysis of the dried residue was a Zeiss - Supra 55VP. The SEM was operated at 15 kV electron beam with around 10 mm working distance.

3.4.1 Sample preparation

All KOH samples collected from the experiments described were collected in plastic sample bottles. These solutions were then diluted down to concentrations of K and Si suitable for analysis by ICP-MS. The amounts of K and Si in these samples before diluting were based on the assumption of a complete reaction described in Equation 17 and the amount of KOH(s)

used when preparing the KOH solutions. The diluted samples were prepared by the use of the reaction sample, 65% HNO₃ and Milli-Q distilled water. The samples were prepared so that the diluted sample had a HNO₃ content of approximately 0.6 mol L⁻¹ comparable to the background used by the ICP-MS.

Dilution of the samples was done with varied amounts in μL of the batch sample according to the strength of the KOH solution used. All samples were weighted on a scale. Preparation was done by dropwise addition of HNO₃ to a weight of approximately 0.859 g followed by pipetting of sample according to the desired dilution factor. Lastly the addition of Milli-Q water was done to a final weight of approximately 15.2505 g. Adjustment in dilution factors was done on a weight basis to take into account the errors from pipetting and dropwise addition.

The complete overview of experiments done is seen in Table 3 where experiment number and corresponding reaction parameters are included. Future referencing of specific experiment numbers are explained by parameters found in this table.

Table 3: Complete overview of the experimental plan showing HCl concentration, amount of Mg₂Si and KOH concentration for every experiment.

Exp. number	Concentration HCl [% (w/w)]	Reactant Mg ₂ Si [mg]	Concentration KOH [mol L ⁻¹]	
3	10	311.7	0.1	} Standard bubbler
4	10	299.1	0.5	
5	10	286.4	1	
6	10	308.4	1.5	
7	10	296.1	2	
8	10	290.1	3	
9	10	293.2	4	
11	10	253.1	1	} Porous bubbler
12	10	293.8	1.5	
13	10	301.0	2	
14	10	299.6	3	
15	10	300.0	2	} Increased Mg ₂ Si
16	10	401.4	2	
17	10	507.7	2	
18	10	600.7	2	
19	7.5	319.5	2	} Increased HCl
21	12.5	291.1	2	
22	15	307.9	2	

4 Results

This section will present the numeric results and the observations obtained from the previously described experiments. The numeric results are calculated from the measurements done by ICP-MS, and the observations will be presented from discoveries done by the author at the time of the experiments. All uncertainty reported originates from the error in the ICP-MS, and the uncertainty is reported as one standard deviation.

4.1 KOH concentration

To start with there was done a test experiment, where 200 mg of Mg_2Si was mixed with HCl and bubbled through 0.09 mol L^{-1} KOH, both the HCl and KOH solution were sent to analysis by ICP-MS. The KOH solution had a Si content corresponding to a $3.2\% \pm 0.1$ yield of the original Si in Mg_2Si . Compared to original amount of elements in Mg_2Si , the HCl solution had a content of $102\% \pm 1\%$ Mg and $15.87\% \pm 0.3\%$ Si.

The first parallel investigated was the effect of increased concentration of KOH with the standard bubbler. The molarity was increased from 0.1 mol L^{-1} to 3 mol L^{-1} , a time after there was done an additional experiment with 4 mol L^{-1} KOH solution. For these experiment only the KOH solution was sent to analysis by ICP-MS. The calculated content of Si show the amounts of Si found in each 200 mL KOH solution taken from the bubbler at the end of each experiment. The calculated Si content in the bubbler given in mg are displayed in Figure 16. The plot shows the varying amount of silicon obtained from gases flowing through the bubbler when the initial amount of Mg_2Si was kept constant at 300 mg and the strength of the bubbler solution was increased. The ICP-MS apparatus always did three measurements of each sample, and calculated a standard deviation for each data point based in the difference between these three measurements. Error bars in the plot show the error related to the ICP-MS analysis procedure. The plot displays a clear increase in silicon uptake for both the blank samples and the real experiments as the KOH concentration was increased. The exception is the

reaction done with 3 mol L^{-1} KOH where there is a small decrease in silicon.

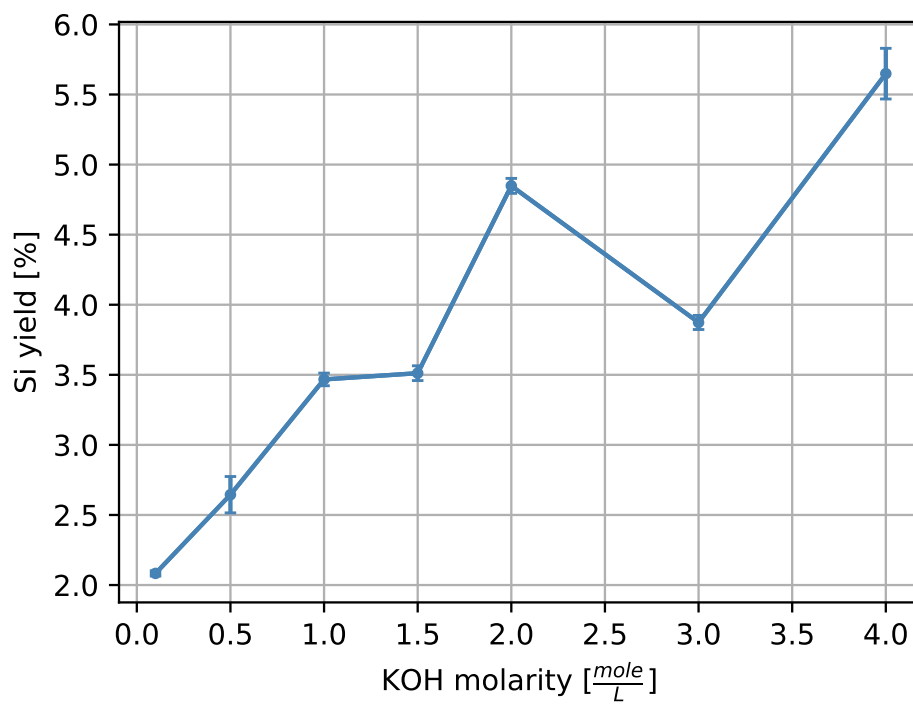
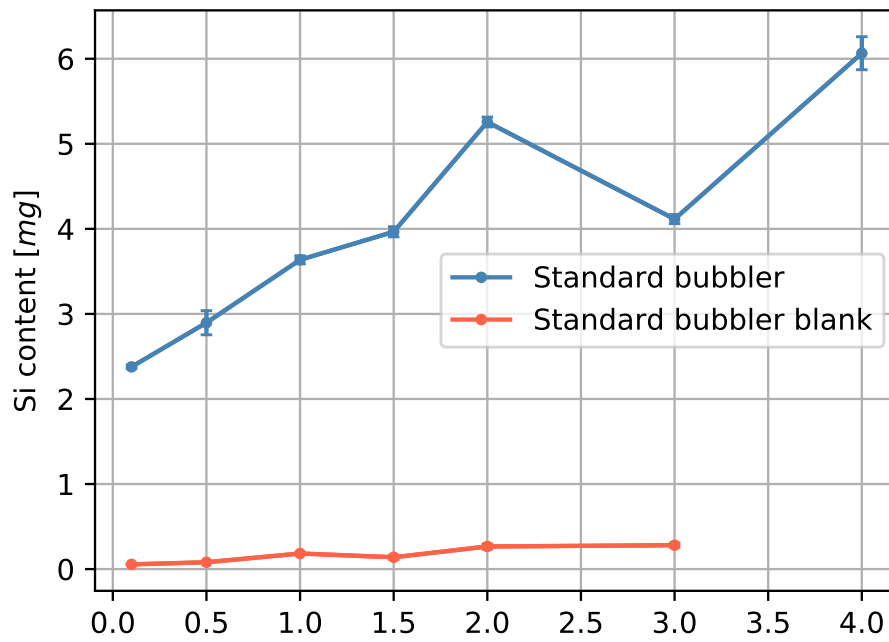


Figure 16: Si content collected in real and blank solution for experiments done with increasing molarity of KOH, corresponding yield to the real experiments are shown in separate y-axis.

For the additional experiment - done a while afterwards - with the largest molarity of 4 mol L^{-1} KOH, Figure 16 shows the further increase in Si content for this last data point. There was not done a blank parallel with this sample. The plot displays a further increase in silicon uptake, the uncertainty from ICP-MS analysis is also significantly higher for the last data point. It is also seen that the collected silicon is significantly higher in the real samples when compared to the blank samples without any reactant Mg_2Si . The content of Si in the blank samples can still be observed to have an increasing trend towards higher molarity of the KOH solution.

The amount of collected Si in the bubbler solution was also compared to the initial amount of Si in the reactant Mg_2Si for each experiment. The resulting yield in % for each experiment can also be seen in Figure 16 where an increasing trend can be observed. The calculated Si yield lies in the range from 2 - 6 %.

4.2 Bubbler porosity

For the second parallel a new bubbler was made by welding on a porous glass tip on the bubbler bottom as seen in Figure 15. The previous experiments with 300 mg Mg_2Si were repeated with this new bubbler for KOH solutions with molarities ranging from 1 mol L^{-1} to 3 mol L^{-1} . Figure 17 shows the resulting Si captured in the bubbler solutions compared to the Si captured by using the standard bubbler.

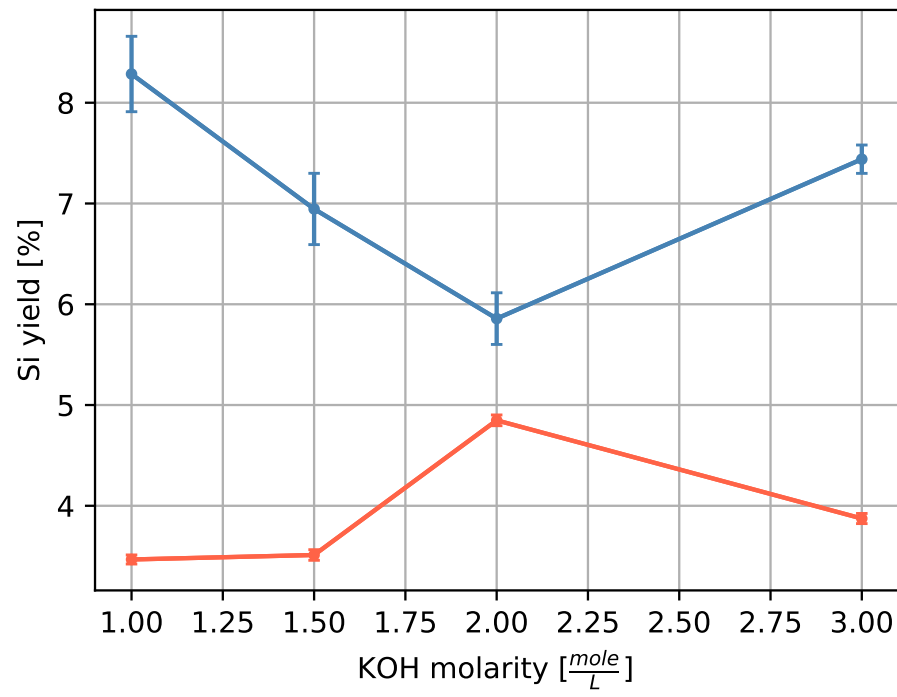
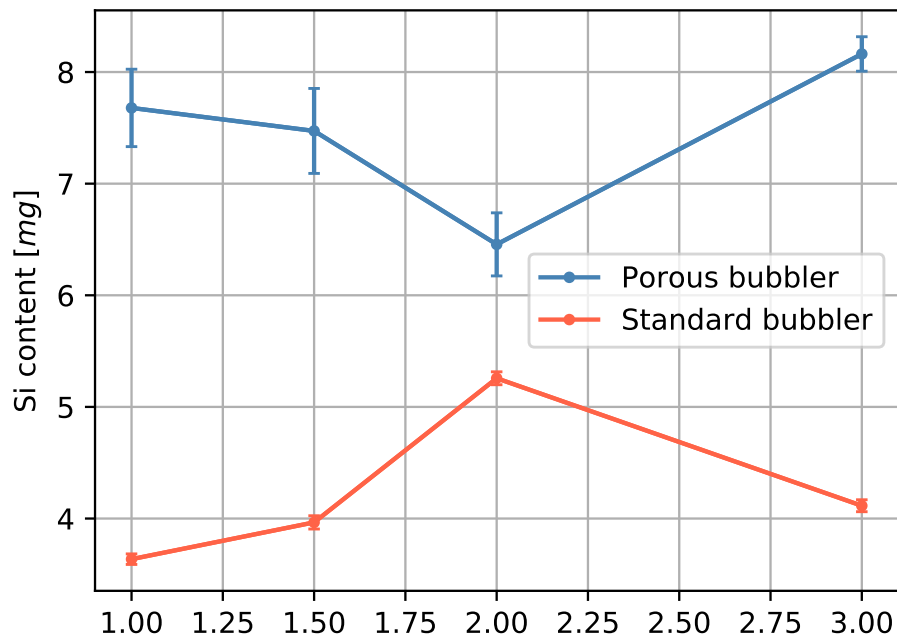


Figure 17: Silicon content collected in increased concentrations of KOH in the porous bubbler compared to the standard bubbler. Corresponding Si yield comparison when compared to original Mg₂Si samples of 300 mg is shown at separate y-axis.

The yield of Si captured by the porous bubbler can also be seen in Figure 17 when compared to that collected by the standard bubbler. The yield of the porous bubbler lies in the range 6 - 8 % compared to 2 - 6 % in the standard bubbler, on average the porous bubbler has higher Si collection than the standard bubbler and therefore also a higher yield. For the porous bubbler there is observed a decrease in Si content towards 2 mol L^{-1} followed by a strong increase when the molarity of KOH is increased further to 3 mol L^{-1} .

4.3 Amount of Mg_2Si

The different amount of Si captured for experiments done with increasing Mg_2Si can be seen in Figure 18. These experiments use the new porous bubbler with KOH and HCl solutions being kept constant at 2 mol L^{-1} and 10 % respectively, the amount of Mg_2Si on the other hand was varied from 300 mg up to 600 mg. The corresponding yield of silicon compared to the content in the original Mg_2Si is observed to have an increase lying in the range 5 - 21%.

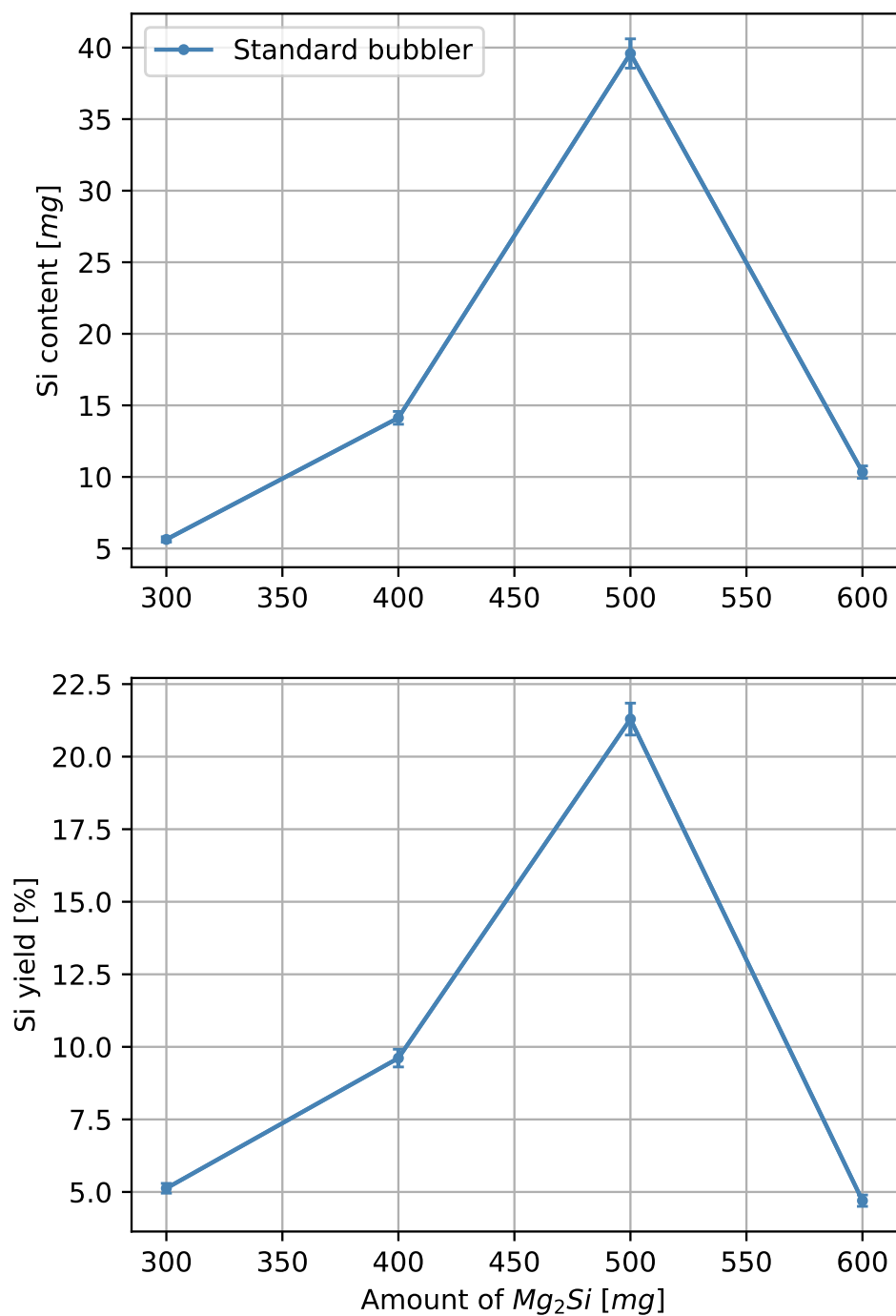


Figure 18: Si content and corresponding yield for experiments done with increasing amount of Mg_2Si by the use of the porous bubbler with constant concentration of 2 mol L^{-1} KOH.

4.4 HCl concentration

The last set of experiments were conducted with the porous bubbler, constant amounts of both Mg_2Si at 300 mg and KOH concentrations at 2 mol L^{-1} . The strength of HCl was varied in the range 7.5 - 15% (w/w). The levels of Si captured by the bubbler solution can be seen in Figure 19. The plotted values show a u-shaped trend in Si content with extremal values of approximately 10 mg of captured Si. The corresponding yield of Si in the experiments done with varying acid concentrations is found in the range of 4 - 8.5% silicon captured from the original silicon entering the reactor as Mg_2Si .

4.4.1 HCl residue

The product solution in the reactor was found to contain a relative large amount of residue at the end of each experiment and was therefore not analysed by ICP-MS for the main experiments. The residue in the HCl solutions was collected by filtering the solutions followed by drying in a heating cabinet. The weight of the residue could then be found and compared to the original amounts of Mg_2Si used in the corresponding experiment. The resulting weight of residue compared to original weight of the Mg_2Si can be seen for all experiments done in Table 4.

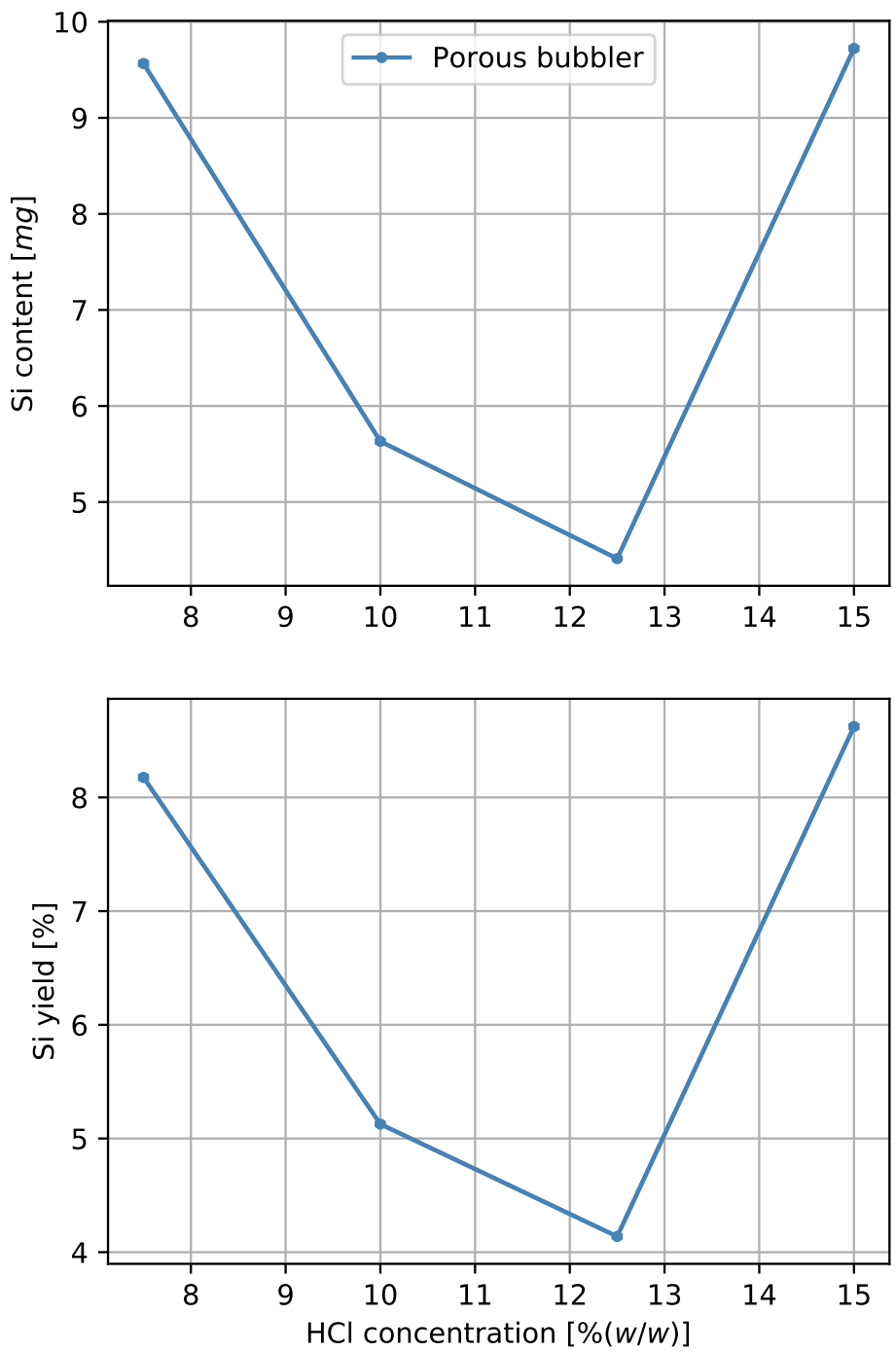


Figure 19: Si content and corresponding yield for experiments done with increasing concentration of HCl by the use of the porous bubbler with constant concentration of 2 mol L^{-1} KOH.

Table 4: Weight of collected residue against original weight of Mg₂Si loaded in each experiment.

Exp. number	Reactant Mg ₂ Si [mg]	Amount of residue [mg]
3	311.7	102
4	299.1	138
5	286.4	128
6	308.4	127
7	296.1	97.0
8	290.1	76.0
9	293.2	80.0
11	253.1	98.0
12	293.8	102
13	301.0	88.0
14	299.6	85.0
15	300.0	110
16	401.4	134
17	507.7	194
18	600.7	175
19	319.5	39.0
21	291.1	96.0
22	307.9	133

The XRD plot of the precipitate collected from the HCl originating from experiment 14 can be seen in Figure 20, the crystalline peaks match those of pure Si. There was also found an amorphous phase that was proposed to be originating from a significant amount of amorphous SiO₂ in the sample.

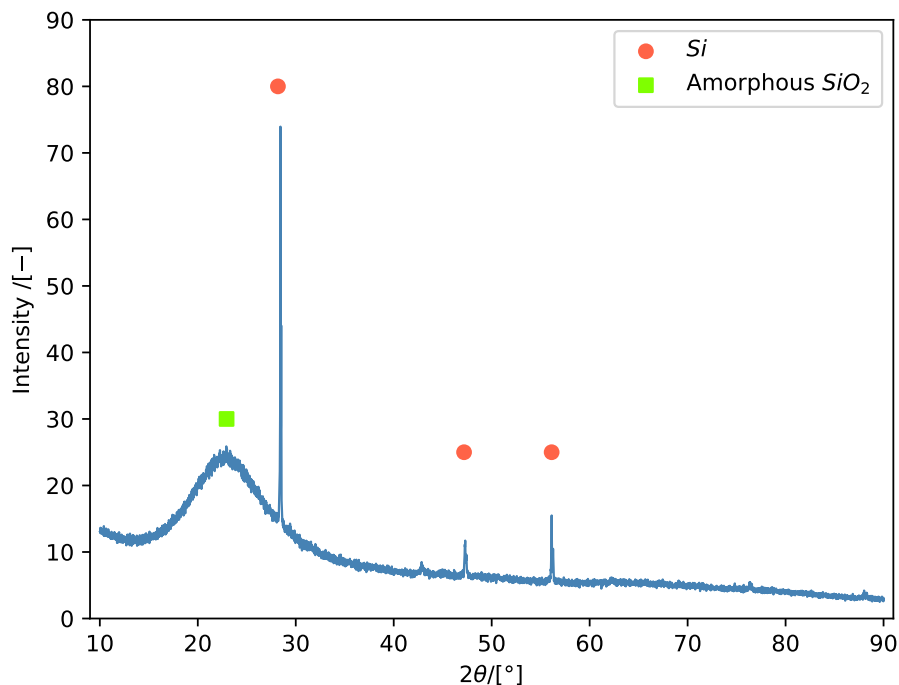


Figure 20: XRD plot of experiment 14, indicated peaks correspond to that of Si and amorphous SiO₂.

The original sample of Mg₂Si was also analysed by the same instrument parameters as the HCl residue and the resulting XRD plot can be seen in Figure 21. The peaks found were confirmed to correspond to those of crystalline Mg₂Si, differing from the reaction residue there was also not found any amorphous phases in this sample. The XRD plot from the Mg₂Si also did not have any of the same peaks as observed in the residue from the reaction in the experiments.

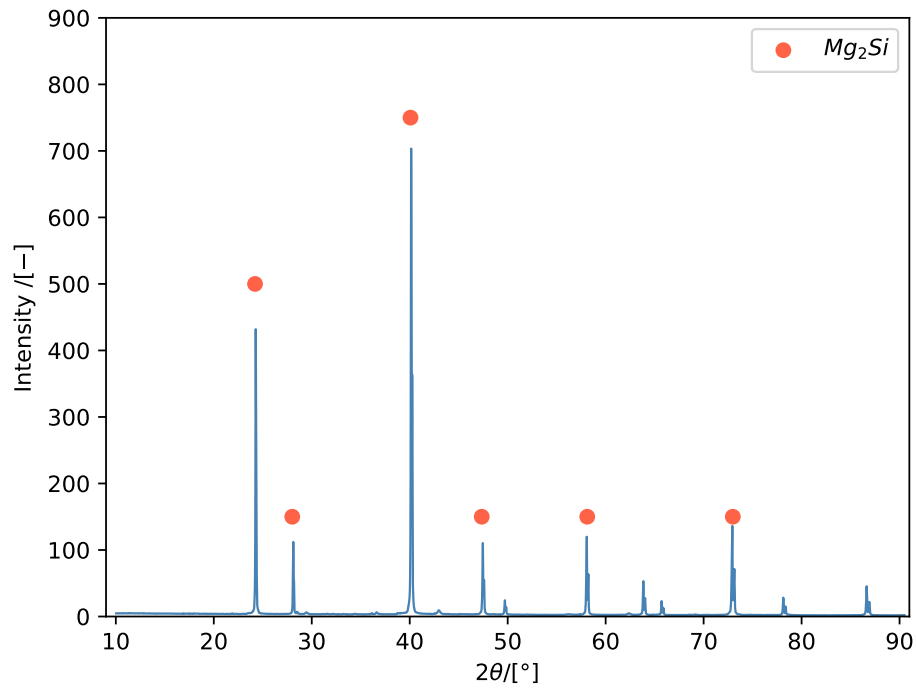


Figure 21: XRD plot of the Mg_2Si powder used for the experiments, indicated peaks correspond to that of Mg_2Si .

To investigate the precipitate further a sample was analysed by SEM to look at phase structure and composition. The resulting image from experiment 17 can be seen in Figure 22 where the phase structure can be seen through secondary electron imaging. The structure is seen as very porous.

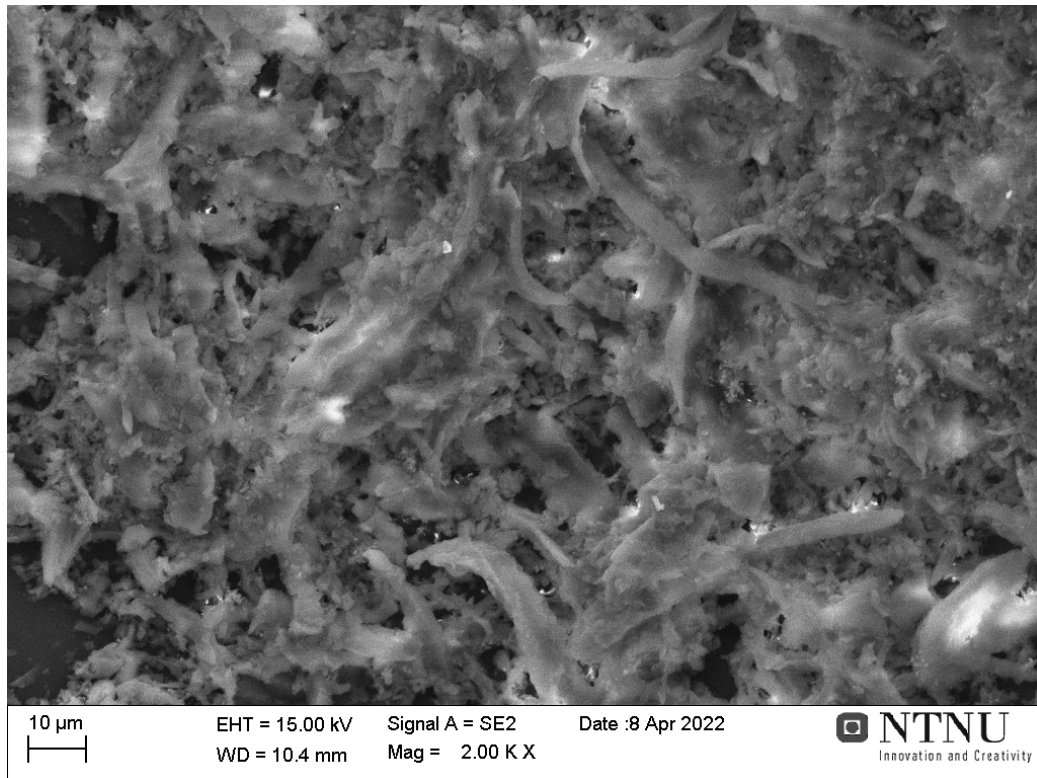


Figure 22: Secondary electron imaging of experiment 17 HCl residue at 2000X magnification.

The same sample viewed by backscattered electron (BSE) imaging can be seen in Figure 23 at 1000X magnification. The BSE imaging shows a sample without clear separation of phases and more uniform distribution of material. As the residue powder was mounted in epoxy some pores can be seen in the sample as well.

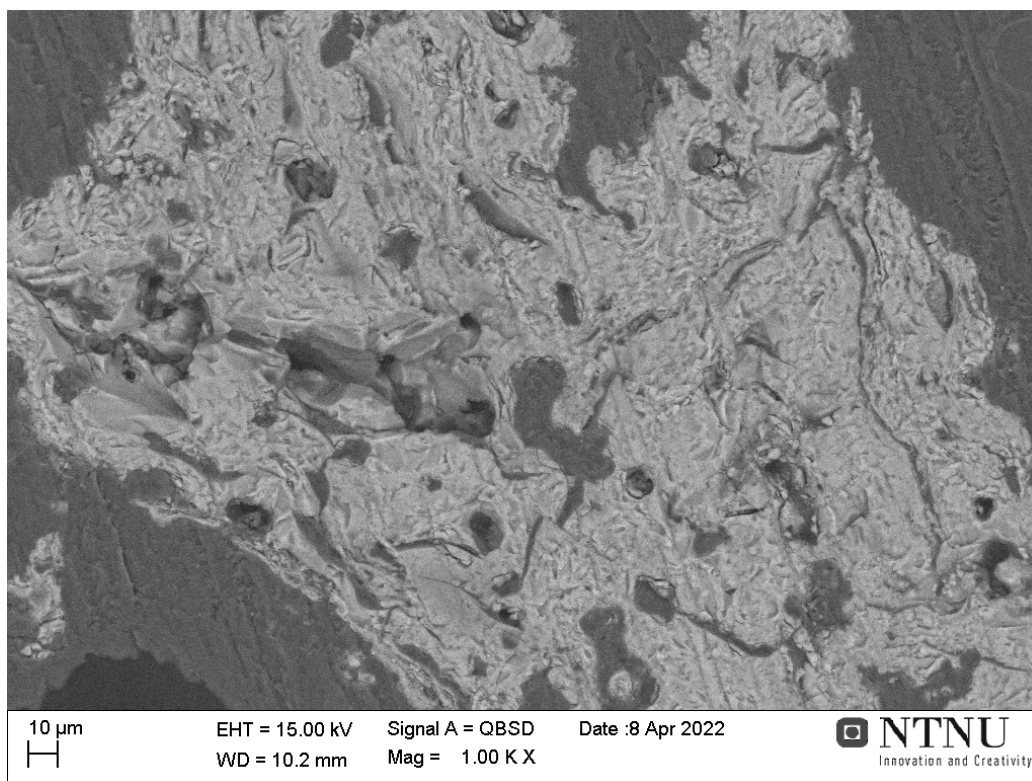
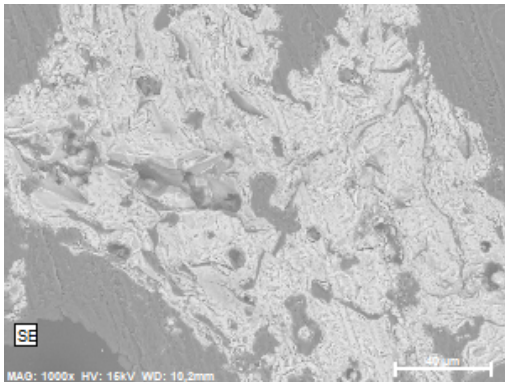


Figure 23: Backscattered electron imaging of experiment 17 HCl residue at 1000X magnification.

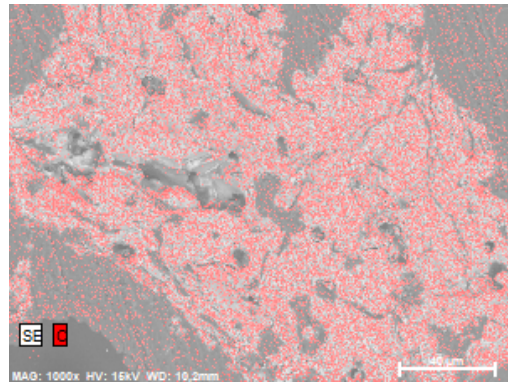
The following X-ray mapping of the precipitate collected from experiment 17 is shown in Figure 24 where it is seen that Si and O are dominant elements in the sample. Mg does not seem to be apparent in the sample at all.

4.5 Observations

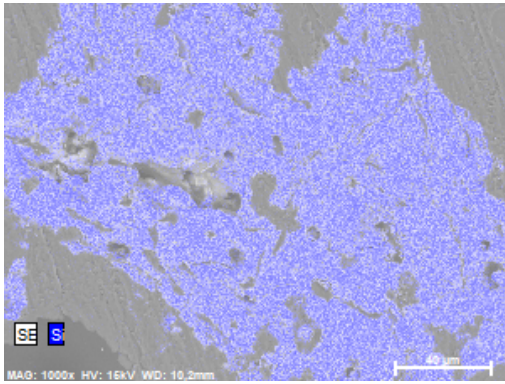
Another noteworthy result is the formation of white coating on the bubbler outlet for several of the experiments as seen in Figure 25. For experiments done at the lower KOH concentrations, there was observed a formation of white dust around the outlet of the bubbler, this was the case for both the standard and the porous bubbler. In the cases of dust formation there was a gradual accumulation of white dust around the outlet from the moment the reaction was initialized. For the experiments with increased Mg_2Si there was



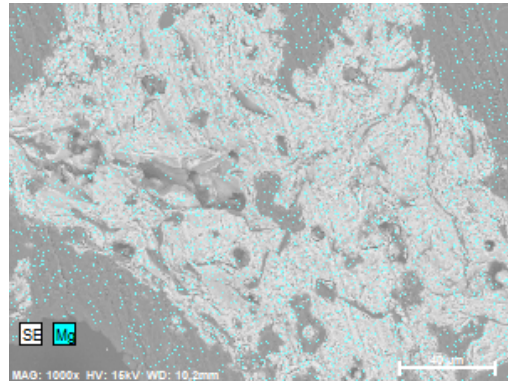
(a) SE image



(b) O image



(c) Si image



(d) Mg image

Figure 24: X-ray mapping of reaction precipitate (experiment 17) at 1000X.

a notable increase in the amount of dust with a crystalline appearance.



Figure 25: Formation of white coating on the outlet of the gas bubbler as seen in several of the experiments done.

In order to get an impression of the reaction there were done many preliminary experiments without any form of quantification of reaction products. The first experiments addressed the addition of small amounts (< 100 mg) of Mg_2Si in water and 10% HCl in an open reactor. The Mg_2Si/H_2O reaction was very slow and completely free from spark or violent gas development. The only visual reaction mechanic was the development of motionless gas bubbles on the Mg_2Si particles.

When added to 10% HCl in oxygen atmosphere, there was an immediate development of white smoke, sparks and bubbles as displayed by Figure 26. Another approach was the addition of concentrated HCl into Mg_2Si powder dissolved in water, resulting in a solution of approximately 10% (w/w) HCl. The interesting result was a significantly reduced amount of sparks, there was also seen a development of foam from the start of the reaction.

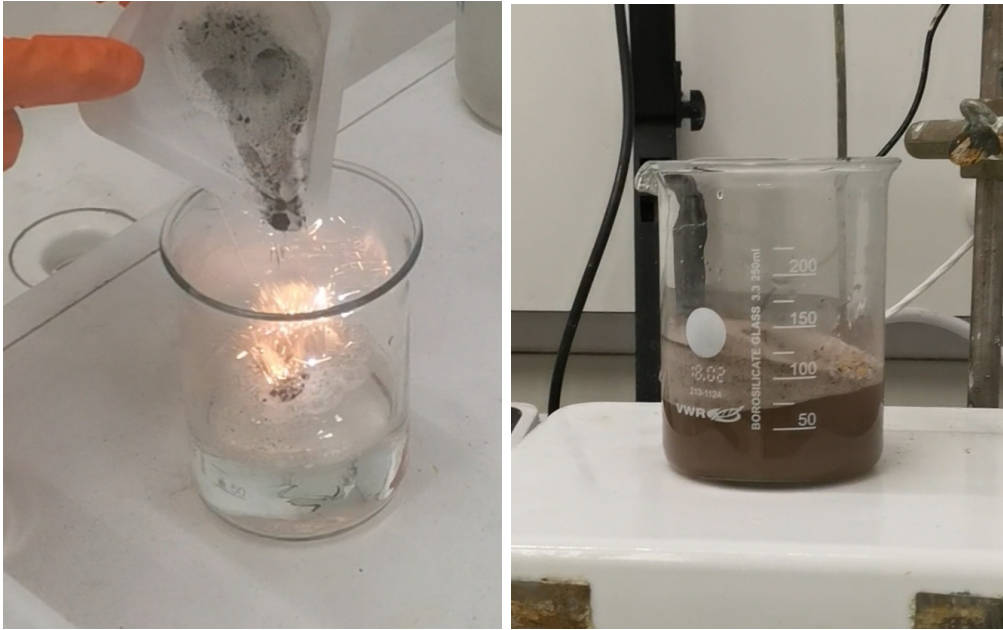


Figure 26: Addition of Mg_2Si in 10% HCl with oxygen present (left). Addition of 36% HCl in $(\text{Mg}_2\text{Si} + \text{H}_2\text{O})$ solution (right).

5 Discussion

This section will discuss the results presented in section 4. The discussion will compare the experimental results and observations with theory and previous literature. An assessment of the uncertainty in the numerical results will also be done throughout the discussion part.

5.1 Variation of reaction parameters

The projects initial goal was to develop a new method so that all silane product gases could be captured in an effective and uncomplicated manner. It was therefore investigated whether a solution of KOH could be used to react with all silane gas so that liquid analysis by ICP-MS could be done to quantify the amount of silane gas formed. The behaviour of the setup was therefore firstly investigated by varying the reaction parameters to see the effect on captured reaction product in the KOH solution. It was clear that the first aspect to investigate was the reliability of the method in catching silane gas, this was done by increasing the concentration of KOH to see if the solutions actually could collect Si from the reaction gas.

A test experiment was done with a relatively weak solution of 0.09 mol L^{-1} KOH, this solution was analysed and found to collect Si corresponding to a yield of 3.2% of the original 200 mg of silicon used. This is a low yield compared to what was found by other authors such as A. Stock (23%)^[31] and Nandi et al. (15%)^[6]. This was also the only experiment where there was done liquid analysis of the HCl solution, the results showed a content of Mg corresponding to $102\% \pm 1\%$ Mg and $15.87\% \pm 0.3\%$ Si. The collected amount of Mg is larger than what we started with, and this could be because of errors caused by the preparation of samples before ICP-MS. The amount of silicon would in that case be tied to the same error.

It is very likely that the magnesium content is more accurate than the amount of silicon. This is because of silicon later found to be present in the precipitate as seen in Figure 20. When preparing the sample for ICP-MS it was hard to pipette a uniform amount solution with precipitate that was later dissolved

with HF. As there was found no Mg in the XRD analysis of the precipitate, it is more likely that it is present as ions in the solution. This is why it is also very likely that the Mg content in the solution is approaching a yield of 100% compared to the Mg content in the original amount of Mg_2Si used for the reaction while the Si yield is much lower due to silicon leaving as silane gas and precipitating as mainly crystalline silicon and amorphous SiO_2 as verified by XRD and SEM analysis.

The continuation of the experiments analysed exclusively the KOH solutions by ICP-MS as a result of the great amount of precipitate in the HCl solutions. The amount of Mg_2Si was also decided to be increased to 300 mg to have a larger scale reaction happening in the reactor and due to the great success in removing oxygen from the reactor making self ignition a minor problem.

5.1.1 KOH concentration

The start of the project was focused on establishing a concentration of KOH in the bubbler solution that could capture all silane gases produced from the reaction between Mg_2Si and HCl. It was therefore very reasonable to keep all reaction parameters constant and increase the bubbler solutions strength until we could achieve levels of Si independent of the increase in KOH molarity. From Figure 16 it is seen that the amount of Si in solution kept increasing with the use of stronger KOH solutions, when the reacting amount of Mg_2Si was kept constant. Based on this result it is very reasonable that there was not established a concentration that was strong enough to react all silane gas into dissolved silicon in solution. The attempt with 4 mol L^{-1} KOH did not reach a plateau either, indicating that none of the KOH solutions could capture all silane gases in the experiments done with the standard bubbler. This was also supported by the observations of white powder coating the bubbler outlet for the lowest concentrations (see Figure 25). Experiments with 3 mol L^{-1} and 4 mol L^{-1} KOH did not have formation of this white coating, this suggests that less silane gases are escaping. Regarding the powders composition it is extremely likely to be the oxidation product of escaped silane gas as the Ar gas would not react with ambient air.

There were several conditions that made it hard to increase the KOH above 4 mol L^{-1} in order to make sure all silane gases were oxidised. ICP-MS was the method of analysis that was chosen for the experiment, and the analysis equipment had a minimum-maximum concentration of 20 ppb - 25 000 ppb for Si and K in solution. For the 300 mg of Mg_2Si used in most of the experiments, the amount of silicon captured from silane gas gets increasingly lowered in the preparation of the KOH solutions ICP-MS. Stronger solutions of KOH requires more dilution in order to fit the accepted levels for the ICP-MS, and this causes extremely low Si levels for the solutions diluted the most, which tends to be more difficult to analyse precisely. One solution to this problem is to produce more silane gas in order to have more silicon in the solutions. The silane producing reaction is extremely exothermic and in combination with the self igniting properties of the silane gases, an up-scaling of the reaction above for instance 1 g Mg_2Si could compromise the safety of the experiments.

It is also seen in Figure 16 that there is a small deviation in the trend with a decrease in silicon content for the experiment done at 3 mol L^{-1} . There are several factors that could be the cause of this, as the dilution step of the samples before ICP-MS was done in only one parallel a large part of the uncertainty can be attributed to this part of the analysis. The instrument has a very high precision in measuring of the samples as displayed by the error bars in Figure 16. An increased uncertainty can also be seen for the last data point for KOH concentration at 3 mol L^{-1} . This is due to the solution having a Si content very close to the lower detection limit of the instrument when analysed. A way to increase the reliability of the results would be to do triplicates when diluting each sample, this would give larger error bars taking into account the uncertainty related to the dilution step.

From Figure 16 it is seen that the KOH solutions collected silicon in solution in a range from approximately 2 - 6 mg. With an initial Mg_2Si amount the yield of Si was in the range from 2 - 5.6%. The results are comparable to that of Nandi et al. which collected silane gas corresponding to yields ranging from approximately 10 - 15%^[6], with the use of 10% HCl in excess.

A yield of maximum 5.6% is very low for the production of silane gas, this may be a result of silane gas escaping the gas bubbler making the yield lower. Another possibility is the fact that not all Mg_2Si will react to form silane gas. Much silicon may still be in the reaction chamber as part of the residue or in solution as ions, a quantification of all content in the HCl solution would have been very beneficial in determining the amount of silicon that escaped the reactor as silane gas when the standard bubbler was in use.

It should also be noted that the content of Si in the blank samples show a weak increase when molarity of KOH is increased. As seen in Figure 16 the Si in the blank samples have a slight increase even though there was no silane gas passing the system. This was beforehand suspected by the use of a glass bubbler, but the effect was thought to be of minimum importance. When compared to the Si content in the experimental samples, the ratios of Si were in the range of 2.3 - 6.8% which indicates that the captured silicon is affected by the use of glass bubblers to a small degree. This is something that can easily be avoided by choosing a material that is not reactive to KOH.

5.1.2 Porous bubbler

It was suggested that the reaction between SiH_4 and KOH could be dependent on the surface interaction between the silane-containing gas bubbles and the solution in the bubbler. The porous bubbler was therefore introduced to increase the bubble surface area significantly. The results from Figure 17 show that the amount of captured silicon on average was significantly higher in the porous bubbler compared to that of the standard bubbler. This is most easily explained by the larger surface area with an increased amount of smaller bubbles compared to few large bubbles in the standard bubbler. It was therefore found to be beneficial to continue using the porous gas bubbler for the rest of the experiments. It was also seen that the lowest concentrations of KOH still had dust formation on the bubbler outlet as seen in Figure 25, this indicates silane gas escaping also from the porous bubbler at similar conditions as the standard bubbler.

The experimental procedure was also modified so that the gas flow was reduced significantly at initiation of the reaction so that the silane gas passed through the KOH solution at a slower rate. It was seen from Figure 17 that the amount of silicon captured was consistently higher when the porous bubbler was used at equivalent experimental conditions. The reaction between KOH and silane gas is because of these results found to be heavily dependent on the way the gas is exposed to the solution. The uncertainty in the values of Si content in the porous bubbler is also much higher. The larger error bars in the plot are from the ICP-MS equipment only, and may be caused by low amounts of silicon in the solutions prepared, making it harder to give precise results. A conclusion that can be drawn from these experiments is that the reaction between gaseous silane and aqueous KOH (e.g. Equation 23) is promoted by higher surface exposure of the gas bubbles.

As seen in both Equation 23 and Equation 24 the hydrolysis of silane gas also liberates hydrogen which also could have been analysed as done by Tan et al. It is seen from Equation 23 that monosilane will react to produce hydrogen gas in the stoichiometric relationship 1:4, quantification of the hydrogen could therefore have been used as well to indirectly measure the amount of silane gas caught by the bubbler solution of KOH.

The experiments done by Tan et al. also used a 30% (w/w) solution of NaOH to quantify SiH_4 indirectly as volume change caused by hydrogen evolution according to Equation 25^[7]. With a density of 1.3311 g mL^{-1} this corresponds to a molarity of approximately 13.3 mol L^{-1} NaOH which is more than double the concentration of the most concentrated KOH solution used in this project. It is possible that using a solution of NaOH could have had a stronger reaction with the silane gas. The use of a concentrated solution like this would also have had increased the chance of oxidising all the produced silane gas, but this solution would not have been possible to analyse by the ICP-MS instrument.

5.1.3 Increasing amount of Mg₂Si

The results from the experiments done with increased amounts of Mg₂Si showed an expected trend of increased Si content in the 2 mol L⁻¹ KOH solutions as displayed by Figure 18. The last data point corresponding to 600 mg has a strong decrease down to 10 mg Si in solution, being an outlier from this trend. This deviation is very likely due to errors attributed to the dilution part prior to the analysis by ICP-MS. As the instrument itself reported a small error in all of the measures it is assumed to be very reliable in terms of reporting realistic values from the samples analysed. The problem is therefore that there was not prepared multiple samples for each experiment done. This would have taken into account the large uncertainty attributed to the dilution part of the experiment.

When looking at the corresponding yield in Figure 18 it is seen that the calculated yield increases with increased amount of Mg₂Si loaded into the reactor. The yield increase up to 21% is also more comparable to that of Stock which achieved a maximum yield of 23%. Although the data may be debatable by the reasons explained before, the increasing trend may be explained by the larger amount and higher concentration of silane gas interacting with the KOH solution. The enhanced gas/liquid interaction can be influencing the Si uptake by same reasoning that switching to a porous bubbler increased the yield compared to the standard bubbler.

5.1.4 Concentration of HCl

The last experimental parameter change was based on the variation in concentration of the HCl solution used in the reaction. The captured Si content can be seen in Figure 19 where a u-shaped trend is observed. The captured silicon lies in the range of 4.5 - 10 mg which is a big variation for the different concentrations of acid. The corresponding yield is ranging from 4 - 8.5%, this is again on average higher yield than that achieved by use of the standard bubbler as seen in Figure 16. The consistency in higher yield with the porous bubbler strengthens the assumption that smaller gas bubbles tends to react

better with the KOH solution.

The effect of changing the HCl concentration is hard to interpret as the trend observed in Figure 19 is of a very ambiguous shape. There is no theory suggesting a decrease in silane production in the range between 7.5 and 15% HCl used for the reaction. Nandi et al. actually experienced an increase in yield when increasing the strength of the acid^[6]. The result seen in Figure 10 displays a silane yield between 10 and 14% opposed to a somewhat lower range of 4 - 8.5% achieved in these experiments. It should also be noted that Nandi expresses HCl concentration in v/v%.

Again the error from the ICP-MS instrument itself delivers an extremely low uncertainty, but as there were only done one parallel of each analysis it is not taken into account the error coming from the preparation done before analysis. The four experiments with increased acid were also done one time only and the results obtained do only account for these specific experiments. Repeating each experiment two-three times would take into account the uncertainty in the performance of each experiment as well. As the performance of each experiment was very time consuming, duplicates were not done and arguable at the expense of the repeatability and accuracy of the experimental results.

5.2 Observations

5.2.1 Preliminary experiments

The observations done in the preliminary experiments were also of great importance. As seen in Figure 26 the addition of Mg₂Si in HCl resulted in momentarily reaction with sparks. When the HCl was added to Mg₂Si mixed in water the reaction was completely different. As the HCl was added some sparks were seen, but of a much smaller degree than before. Most interestingly was the formation of foam, this could be because of a reaction happening completely surrounded by water not allowing the gas to escape easily and therefore appearing as a cluster of gas bubbles with silane gas. The interaction between liquid acid and solid Mg₂Si powder could therefore be

very critical when optimizing the amounts of gas produced by the reaction. It is also possible that the yield of the experiments are inhibited by the water present in the acid solution as suggested by Nandi et al^[6].

5.2.2 SiO₂ dust formation

The formation of white coating on the bubbler outlet as seen in Figure 25 is very likely the oxidation of silanes when finally coming in contact with air. White SiO₂ as reaction product is therefore seen as a layer specifically on the outlet as this is the first position in the reaction setup where the oxidation reaction of silane with O₂ is possible. This result is also a good cue of whether all silane has been oxidised by the KOH or if some has gone through the bubbler and reacted with ambient air instead.

5.3 Analysis

5.3.1 HCl solutions

The product solution from the reaction between Mg₂Si and HCl was not analysed in this project because of the large amount of precipitate in each sample. To inspect these solutions with ICP-MS a large amount of HF would have had to be used to dissolve all elements into solution. On the other hand the precipitate has been filtered to be analysed by X-ray powder diffraction in order to characterize the solid reaction products. It was first anticipated that the residue would contain larger amounts of precipitated magnesium compounds as explained by the theory. It was thought that magnesium would be dominant in the residue mostly as Mg(OH)₂ because of its low solubility at 6.4 mg L⁻¹ H₂O at 25 °C. MgCl₂ on the other hand is very soluble with a solubility of 0.543 kg L⁻¹ H₂O at 20 °C and would likely be more present in the solution. Since the reacting Mg₂Si was of relative small amounts this may be the cause of no Mg in the residue^[38].

The residue from each HCl solution was collected and dried, the calculated amount of precipitate from each experiment is shown in Table 4 together with the original amount of Mg₂Si used in each sample. There is a big variance

in the amount of collected residue, but compared to the original weight of mainly 300 mg Mg_2Si approximately one third of the weight is collected as dried precipitate from each experiment. It is evident that a large part of the reaction product ends up as precipitate after the reaction.

5.3.2 X-ray powder diffraction and Scanning Electron Microscopy

The XRD analysis of the precipitate revealed that it was composed of mainly Si mixed with an amorphous phase that had good fit with that of SiO_2 . The X-ray mapping done in SEM also revealed that the phases contained Si and O exclusively as seen in Figure 24. It is therefore very likely that the precipitate consists of a mixture of pure silicon with amorphous silica. The results from XRD seen in Figure 20 were consistent for three independent samples in showing the peaks corresponding to crystalline silicon. An amorphous phase of what was found to be silica was also observed. The discovery of silicon is very interesting as the solid reaction products from the literature review were expected to be mostly $\text{Mg}(\text{OH})_2$ because of its low solubility in water. Polycrystalline silicon is also insoluble in water, which supports the findings from XRD.

5.3.3 Dilution of samples

The ICP-MS used for quantitative analysis had a theoretical minimum and maximum analysis thresholds of 20 and 10 000 ppb respectively for all elements. For spectator elements the maximum thresholds could be extended to 25 000 ppb. Dilution of samples for ICP-MS was therefore done with respect of these thresholds, and content of Si and K was calculated on the assumption of 100% conversion of the reactions described in Equation 17 and Equation 23. The amount of K was calculated from the molarity of the KOH solution used in each experiment.

As the solutions of KOH were made more concentrated, the dilution factor had to be increased to have a satisfying concentration for ICP. The increased dilution was done on the expense of the amount of Si in the samples, as this content was significantly lower than that of the K. This effect was

very noticeable at higher concentrations of KOH at for example 3 mol L^{-1} where the prepared sample had an estimated K content of 25 000 ppb and Si content of 100 ppb, very close to the minimum analysis threshold of the ICP. Increasing the KOH strength beyond 3 mol L^{-1} in experiments was therefore difficult without increasing the reacting amount of Mg_2Si significantly, which again could compromise the safety of the experiments done.

The problem of big concentration gap between Si and K made this analysis method practically limited to KOH concentrations up to approximately 3 mol L^{-1} even though concentrations up to 5 mol L^{-1} and higher were desired to have a better understanding of the effect of increased KOH concentration on the uptake of Si from reaction product gases. When related to the results from Figure 16 it is seen that the amount of Si captured with increasing concentrations of KOH had a strong increase. The second last data point corresponding to the strongest solution of KOH shows a deviation from this trend, and this is most likely due to experimental errors done in the dilution process. The dilution factor had to be increased due to the high concentration, but the analysis done by ICP-MS showed good reliability even though the Si content was very close to the instruments minimum threshold.

5.4 Method feasibility

KOH was used in a gas bubbler as a method of decomposing gaseous silane (SiH_4 , Si_2H_6 , Si_3H_8) to solution before analysing by the use of ICP-MS. The use of this method is both advantageous and disadvantageous in the examination of the gas product from the reaction between Mg_2Si and HCl.

Advantages of using KOH in different concentrations are that this allows us to measure the amount of silane gas formed from the Mg_2Si and HCl reaction in a very simplistic manner. Assuming that all of the silane gas decomposes into silicon ions in solution, the solution is analysable by ICP-MS. The amount of silicon in the KOH solution can be used as an indirect method of measuring the silane production in accordance to Equation 23 and Equation 24 without the need of gas analysis equipment that has to be customized for this specific

reaction setup. The use of KOH is also relatively easy to perform and does not involve advanced method developed for gas-analysis. This method will also allow us to calculate the reaction conversion percentage by comparing amount of Si in the Mg_2Si with that of the Si in KOH-solution.

The big disadvantage with this setup is that there is no way of separating the formation of different silane species being mainly SiH_4 and Si_2H_6 . To do this there has to be developed a method of specific reduction for each compound. A more sophisticated method would be to do gas analysis by equipment such as either FTIR, mass spectrometry or gas chromatography. This would help distinguish the different gases produced, and it would also possibly strengthen the results obtained by ICP-MS analysis of the aqueous KOH solutions.

Another disadvantage is the problem related to the use of KOH where there is a need for dilution before ICP-MS analysis. Higher concentrations of KOH needs a stronger dilution before analysis which dilutes the relative small amount of Si into extremely small concentrations down to around 20 ppm. As explained before this limits the method to analysing KOH solutions up to approximately 3 mol L^{-1} for this specific setup.

5.5 Reaction parameters

There are still important reaction parameters to be investigated related to the presented reaction setup. Substituting the oxidising solution in the bubbler and increasing the temperature are two factors that could be crucial in ensuring that all silane gas is oxidised and captured into the solution. Strong aqueous oxidants such as NaOH could be able to convert all silane gases into dissolved silicon at even lower concentrations, possibly evading the difficulty of a large gap between Si and K in solution. The reaction setup used in this project has also been operated completely without risk scenarios. It would therefore have been possible to investigate larger amounts of Mg_2Si as the possible amounts of gases produced as silane are still safe.

6 Conclusion

The reaction setup has successfully captured silicon from silane gas produced by Mg_2Si powder reacted with aqueous HCl . The main conclusions drawn from the results are:

- A method of indirect gas analysis has been developed and proven to be an alternative way of measuring silane gas compared to direct gas analysis.
- The reaction between silane gas and KOH is highly dependent on the interaction between the gas bubbles reactive area and aqueous KOH in the gas bubbler.
- There is a relationship of stronger reactivity between the silane gases and the KOH solution with increasing concentration of KOH .
- There is an uncertainty in the numeric result that is mostly attributed to the dilution step of samples before ICP-MS. This could have been minimised by doing multiple dilution parallels of each experiment.

6.1 Future work

- This thesis has been part of a project where the objective has been to investigate the possibilities of a new production route from quartz raw material to pure silicon of solar grade purity. Earlier studies have produced Mg_2Si from the magnesiothermic reduction of silica in a tube furnace, the next step would be to investigate the reaction between NTNU-produced Mg_2Si and HCl with the intention to produce silane gas in an energy efficient manner.
- To have a greater understanding of the reaction as a whole there should be done a silicon mass balance of the reaction taking into account silicon inserted as Mg_2Si and ending as a part of reaction precipitate, silane gas captured by KOH and as gas escaped through the bubbler. The product HCl solutions should also be analysed in order to determine the amount of Si in solution.
- There is also a need to investigate the thermodynamics of the acid treatment of Mg_2Si . Future work should focus on determining how much theoretical amount of silane gas that is obtainable for this reaction and if the reported yields are somewhat close of the theoretical maximum.
- As proposed there should be investigated if other oxidants can be used in the bubbler such as NaOH . Substituting other reaction materials of the setup such as type of acid is also an approach that can increase the amount of silane gas produced.
- There is still a wide range of reaction parameters that can be investigated. An increase in Mg_2Si as well as investigating the temperature dependence of the $\text{Mg}_2\text{Si} + \text{HCl}$ reaction are some of the possibilities.

7 References

- [1] SolarPower Europe. Global market outlook for solar power 2021-2025. 2021.
- [2] A. Schei, J. Tuset, and H. Tveit. Production of high silicon alloys. 1998.
- [3] URL https://en.wikipedia.org/wiki/Ellingham_diagram. [Accessed 10. June 2021].
- [4] S. Zheng, A. Engh, M. Tangstad, and X. Luo. Numerical simulation of phosphorus removal from silicon by induction vacuum refining. *Metallurgical and Materials Transactions A*, 2011. doi: 10.1007/s11661-011-0621-3.
- [5] G. Fisher, M. R. Seacrist, and R. W. Standley. Silicon crystal growth and wafer technologies. 2012. doi: 10.1109/JPROC.2012.2189786.
- [6] K. Nandi, D. Mukherjee, A. Biswas, and H. Acharya. Optimization of acid concentration, temperature and particle size of magnesium silicide, obtained from rice husk, for the production of silanes. 1993. doi: 10.1007/BF00506325.
- [7] Z.H. Tan, L.Z. Ouyang, J.M. Huang, J.W. Liu, H. Wang, H.Y. Shao, and M. Zhu. Hydrogen generation via hydrolysis of mg₂si. 2019. doi: <https://doi.org/10.1016/j.jallcom.2018.08.122>.
- [8] A. Jäger-Waldau. Snapshot of photovoltaics - march 2021. *EPJ Photovoltaics*, 2021. doi: 10.1051/epjpv/2021002.
- [9] W.O. Filtvedt, A. Holt, P.A. Ramachandran, and M.C. Melaaen. Chemical vapor deposition of silicon from silane: Review of growth mechanisms and modeling/scaleup of fluidized bed reactors. *Solar Energy Materials and Solar Cells*, 2012. doi: <https://doi.org/10.1016/j.solmat.2012.08.014>.
- [10] K. Aasly. *Properties and behavior of quartz for the silicon process*. NTNU, Trondheim, 2008.

- [11] K. F. Jusnes. *Phase transformations and thermal degradation in industrial quartz*. NTNU, Trondheim, 2020.
- [12] J. Safarian, G. Tranell, and M. Tangstad. Processes for upgrading metallurgical grade silicon to solar grade silicon. *Energy Procedia*, 2012. doi: <https://doi.org/10.1016/j.egypro.2012.03.011>.
- [13] U.S. Department of the Interior. Silicon data sheet - mineral commodity summaries 2020. 2020.
- [14] H. Zhang, Z. Chen, W. Ma, S. Cao, K. Jiang, and Y. Zhu. The effect of silica and reducing agent on the contents of impurities in silicon produced. 2021. doi: 10.1007/s12633-021-01072-w.
- [15] J.E.A. Maurits. Chapter 2.6 - silicon production. In *Treatise on Process Metallurgy*, pages 919–948. Elsevier, Boston, 2014. ISBN 978-0-08-096988-6. doi: <https://doi.org/10.1016/B978-0-08-096988-6.00022-5>.
- [16] G. Tranell, I. Kero, and S. Grådahl. Airborne emissions from si/fesi production. 2017. doi: 10.1007/s11837-016-2149-x.
- [17] E. Pastor Vallés. Life Cycle Assessment of silicon metal by aluminothermic reduction: an industrial symbiosis approach. Master’s thesis, NTNU, 2021.
- [18] E. Nordgård-Hansen and K. Hildal. Skull formation in dynamic modelling of silicon refining. 2016. doi: 10.1016/j.ifacol.2016.10.116.
- [19] Z. Xing, J. Lu, and X. Ji. A brief review of metallothermic reduction reactions for materials preparation. 2018. doi: 10.1002/smt.d.201800062.
- [20] H. Fathi. Metallothermic reactions - past, present and future. 2018.
- [21] K. Yasuda and T. Okabe. Solar-grade silicon production by metallothermic reduction. 2010. doi: 10.1007/s11837-010-0190-8.
- [22] S. E. Sadique. Production and Purification of Silicon by Magnesiothermic Reduction of Silica Fume. Master’s thesis, University of Toronto (Canada), 2010.

- [23] M. Barati, S. Sarder, A. McLean, and R. Roy. Recovery of silicon from silica fume. 2010.
- [24] K. Larbi. Synthesis of high purity silicon from rice husks. 2010.
- [25] B. S. Xakalashie. Removal of phosphorus from silicon melts by vacuum refining, 2012.
- [26] D. Yang. *Handbook of Photovoltaic Silicon*. Springer Berlin Heidelberg, 1st ed. 2019 edition, 2019. ISBN 978-3-662-56471-4,978-3-662-56472-1. URL <http://gen.lib.rus.ec/book/index.php?md5=6b3ae40d40dec52e79c53b9c55444d8a>.
- [27] A. Jäger-Waldau. *1.09 - Overview of the Global PV Industry*. Elsevier, Oxford, 2012. ISBN 978-0-08-087873-7. doi: <https://doi.org/10.1016/B978-0-08-087872-0.00110-4>.
- [28] W.O. Filtvedt, A. Holt, P.A. Ramachandran, and M.C. Melaaen. Chemical vapor deposition of silicon from silane: Review of growth mechanisms and modeling/scaleup of fluidized bed reactors. 2012. doi: <https://doi.org/10.1016/j.solmat.2012.08.014>.
- [29] R. E. Kirk, D. F. Othmer, M. Grayson, D. Eckroth, et al. *Kirk-Othmer Encyclopedia of Chemical Technology*. Wiley-Interscience, 4th edition edition, 2004.
- [30] Walter Simmler. *Silicon Compounds, Inorganic*. John Wiley & Sons, Ltd, 2000. ISBN 9783527306732. doi: <https://doi.org/10.1002/14356007.a24.001>.
- [31] A. Stock. *The Hydrides of Boron and Silicon*. Cornell University Press, Ithaca, New York, 1933.
- [32] W. C. Johnson and S. Isenberg. Hydrogen compounds of silicon. i. the preparation of mono- and disilane. 1935. doi: [10.1021/ja01310a053](https://doi.org/10.1021/ja01310a053).
- [33] M. Zhu, A. Azarov, E. Monakhov, K. Tang, and J. Safarian. Phosphorus separation from metallurgical-grade silicon by magnesium alloying and acid leaching. 2020. doi: <https://doi.org/10.1016/j.seppur.2020.116614>.

- [34] R. Schwarz and E. Konrad. Über den reaktionsmechanismus der silanbildung aus magnesiumsilicid (i.). 1922. doi: <https://doi.org/10.1002/cber.19220550938>.
- [35] T. C. Frank., K. B. Kester, and J. L. Falconer. Catalytic formation of silanes on copper-silicon alloys. 1985. doi: [https://doi.org/10.1016/0021-9517\(85\)90286-6](https://doi.org/10.1016/0021-9517(85)90286-6).
- [36] G. M. Wyller., T. J. Preston, S.G. Anjitha, M. O. Skare, and E. S. Marstein. Combination of a millimeter scale reactor and gas chromatography-mass spectrometry for mapping higher order silane formation during monosilane pyrolysis. 2020. doi: <https://doi.org/10.1016/j.jcrysgro.2019.125305>.
- [37] J.-R. Chen, H.-Y. Tsai, S.-W. Wang, S.-Y. Wu, E. Y. Ngai, and K. P.-P. Huang. Ignition characteristics of steady and dynamic release of pure silane into air. 2010. doi: 10.1007/s10573-010-0053-1.
- [38] International Labour Organization, 2022. URL https://www.ilo.org/dyn/icsc/showcard.display?p_version=2&p_card_id=0764. [Accessed 28. March 2022].

A Calculation of Si yield

Equation used to calculate silicon yield from each experiment shown in Equation 26

$$\% \text{ Silicon yield} = \frac{\text{Amount of Si in KOH [mg]}}{\text{Amount of Mg}_2\text{Si [mg]} \cdot \frac{28.09}{76.7}} \cdot 100\% \quad (26)$$

An example could be initial 300 mg Mg₂Si and a final KOH solution analysed and found to contain 10 mg Si. Calculated yield would then be 9.10% as shown by Equation 27.

$$\% \text{ Si yield} = \frac{10 \text{ mg}}{300 \text{ mg} \cdot \frac{28.09}{76.7}} \cdot 100\% = 9.10\% \quad (27)$$